Salt structures and salt tectonics in the Barents Sea

Southwestern sub-basin, Nordkapp Basin

Ha Thi Thanh Hoang

Master Thesis in Geosciences
Petroleum Geology and Petroleum Geophysics
30 credits

Department of Geosciences
Faculty of Mathematics and Natural Sciences

UNIVERSITY OF OSLO
June 2016

ACKNOWLEDGEMENT

I would like to express my sincerest gratitude to my supervisors, Professor Roy Helge Gabrielsen, and Professor Jan Inge Faleide, for being excellent supervisors. Their encouragement, patience, and invaluable suggestions as well as knowledge made this work successful. Moreover, I would like to thank Dr. Michel Heereman who helped in data management.

I would like to acknowledge TGS/Fugro & NPD for providing the seismic and well data for this study.

I would like to acknowledge Schlumberger for making Petrel available.

I am deeply and forever indebted to my family for their love, support and encouragement throughout my entire student life.

I owe many thanks to friends who helped and supported me during doing and writing of this thesis.

ABSTRACT

Fault systems, salt structures and halokinetic sequences of Near Top Permian – Base Cretaceous succession are interpreted on 2D seismic data located in the southwestern sub-basin of the Nordkapp Basin of the southwestern Barents Sea.

The SW Nordkapp Basin is surrounded by the Nysleppen and Måsøy fault complexes and flat-lying platforms. It was formed in a regional rift phase in Late Devonian to Carboniferous time. Bounding faults of the Nysleppen Fault Complex defining the northwestern boundary have the general trend of NE-SW. They are planar normal faults dipping towards the SE with a large vertical separation. In contrast, the Måsøy Fault Complex defining the southeastern margin consists of ENE-WSW trending faults. They are similar to those of the Nysleppen Fault Complex. However, the vertical displacement is much smaller than that of the Nysleppen Fault Complex. Therefore, the rift phase in Late Devonian to Carboniferous created a basin having an asymmetric configuration with a larger subsidence along the northwestern margin.

The second rift phase occurred in Middle Jurassic to Base Cretaceous. Faults of the Nysleppen Fault Complex strike NE-SW. Several fault segments at the Norsel High trend NNE-SSW. The Nysleppen Fault Complex consists of two series of fault with opposite dip-direction. Bounding faults dip towards the NE. The Måsøy Fault Complex dips towards the SW. The basin was more symmetric. Most of bounding faults active this period are listric normal faults with much smaller vertical separation compared with those of the previous rift phase. Some faults related to salt pillows are rotated and curved in the map view.

Salt diapirism plays an important role in the basin. A widespread evaporite layer was accumulated in the latest Carboniferous-earliest Permian time in the SW Barents Sea, including the SW Nordkapp Basin. The calculation indicates the original salt layer in the SW Nordkapp Basin had an average thickness of approximately 1.2 km. Based on the observation and interpretation of 2D seismic data, salt is found in two structural settings: (1) as stocks and walls in the basin, and (2) pillows along the basin margins, associated with fault complexes. Salt structures vary in size and maturity.

The Near Top Permian to Induan (Early Triassic) succession was deposited with the thickness thinning towards salt structures in the basin. It indicates the deposition of sediment in the primary rim syncline formed due to salt movement in the pillow stage. Differential loading resulted from the rapid deposition of a huge amount of clastic sediment from the north is

suggested to be the main cause because there is no evidence of tectonic activity at that time. The period of Induan – Olenekian (Early Triassic) is the main phase of salt movement with large rim synclines, development of growth strata. The Olenekian – Middle Jurassic succession was deposited when the salt movement was in the late stage. Salt structures have a widening shape. Salt diapirsm stopped and the succession of Middle Jurassic – Base Cretaceous was deposited with a relatively constant thickness.

Salt pillows are believed to be formed and developed during the period of Induan – Middle Jurassic. The thickness of the succession decreases towards the crest of salt pillow. It is a presence of faults related to salt pillows. The movement of salt pillows towards the basin created deformation and collapse of surrounding strata and faults.

Table of Contents

1. INTRODUCTION

The Barents Sea is located in the northwestern corner of the Eurasian shelf (Glørstad-Clark et al., 2010). Geographically, it lies between Norway and Russia in the south, Svalbard towards the northwest, and Novaya Zemlya towards the east (Figure 1.1). Since the Caledonian orogenic movement ended in Early Devonian, the Barents Sea has been affected by several stages of tectonics (Gabrielsen et al., 1990).

The study area is situated in the Nordkapp Basin, the southwestern part of the Barents Sea (Figure 1.1). Since the 1980s, the Nordkapp Basin has become an attractive area for hydrocarbon exploration. During geologic evolution of the Nordkapp Basin, halokinetic movement played an important role in tectonic styles and sedimentation (Gabrielsen et al., 1990). Halokinesis is important for creation of structural traps, stratigraphic traps as well as controlling the distribution of reservoirs and their quality around salt structures (Archer et al., 2012). Therefore, an understanding of salt's behaviour and its role is crucial for future petroleum exploration purposes in such a salt-related basin as the Nordkapp Basin.

The main purpose of the master thesis is to contribute to a better understanding of the development of salt structures and salt tectonics in the Nordkapp Basin, specifically its southwestern part. The study data consists of two dimensional (2D) seismic and well data.

Based on the detailed observations and the seismic to well correlation, it is possible to define the deposition of sediment and its relationship to the structural development as well as the timing and causes of salt movement. Previous published works were utilized in order to help explain the tectonic and depositional history of the basin.

.

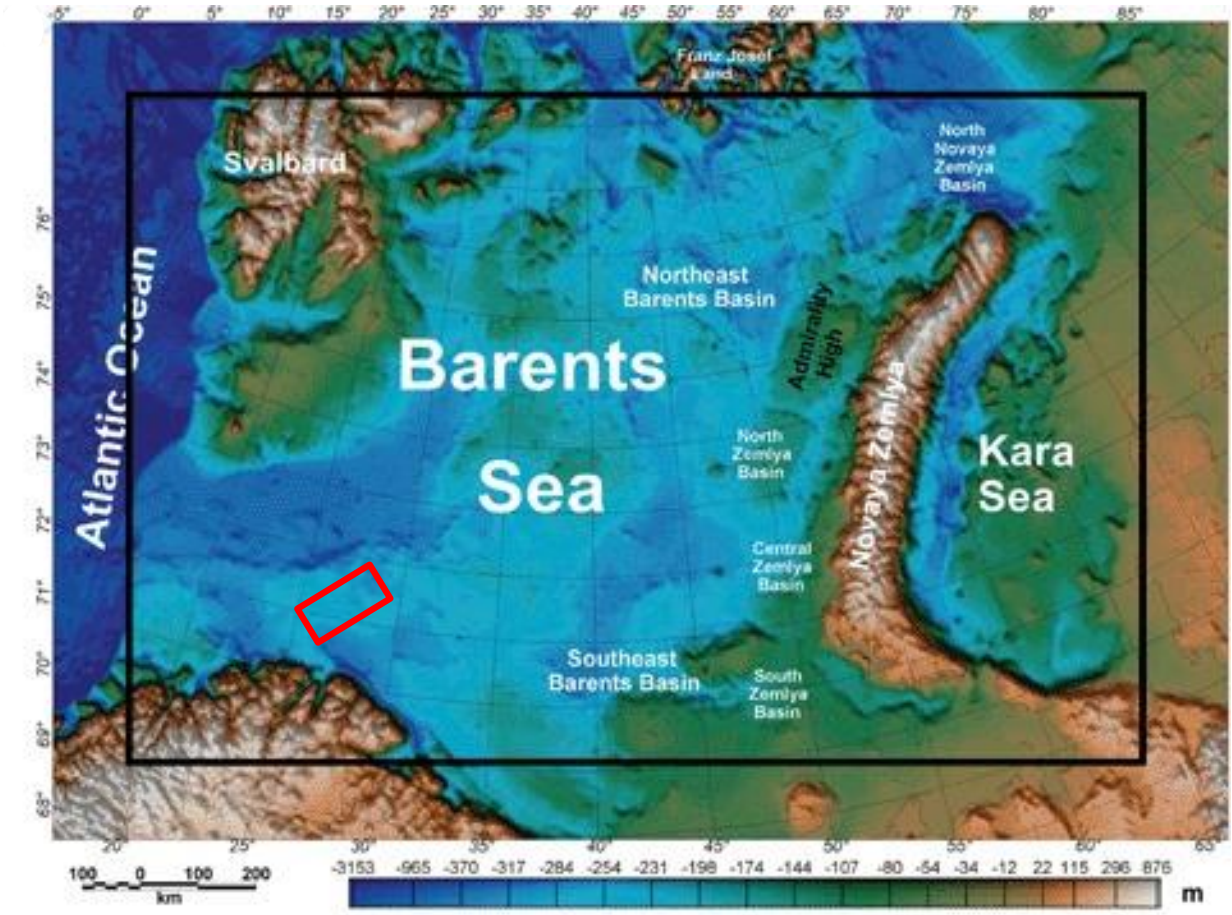

Figure 1.1 Map showing topography/bathymetry of the Barents Sea. The location of the study area is outlined by the red rectangle (modified from Ebbing (2009)).

2. GEOLOGICAL FRAMEWORK

The regional geology of the Barents Sea has been documented in many studies throughout the years Faleide et al. (1984); Gabrielsen et al. (1990); Faleide et al. (1993); Johansen et al. (1994); Faleide et al. (1996); Gudlaugsson et al. (1998); Worsley et al. (2008); Faleide et al. (2010); Glørstad-Clark et al. (2010); Faleide et al. (2015).

2.1 The Barents Sea's geological evolution

Following the Caledonian orogeny in the Late Silurian to Early Devonian, sediments were exposed and eroded (Smelror et al., 2009). The Barents Sea experienced a major rift event in the Late Devonian to the Carboniferous. The compressional regime characterizing the Caledonian orogeny changed to extension. The rift resulted in the formation of extensional basins and highs with bounded faults (Faleide et al., 2010). The Nordkapp Basin was one of the basins which were formed during this rift event (Gudlaugsson et al., 1998). Fault movements ceased in the eastern area at the end of the Carboniferous. A period of calm tectonic activity was in the eastern area of the Barents Sea. The western area was affected by renewed faulting, uplift and erosion in the Permian to Early Triassic time (Faleide et al., 2010).

The Triassic to Early Jurassic is considered a relatively quiet period in terms of tectonics (Gabrielsen et al., 1990). A regional rift phase started in the late Middle Jurassic. It increased in intensity during the Late Jurassic-Early Cretaceous time. Another rift event occurred in the Early Cenozoic time. It was followed by the uplift and massive erosion in the Neogene (Gabrielsen et al., 1990). It was related to the post-glacial development in the northern hemisphere in the Late Pliocene to Pleistocene/Holocene (Faleide et al., 2010).

Two rifting phases in the late Mesozoic and Cenozoic time has affected the western part of the Barents Sea strongly. In contrast, the eastern part has experienced less pronounced tectonic activity (Gabrielsen et al., 1990). Since the end of the Carboniferous, it has been characterized by relatively stable platforms. Moreover, salt tectonics influenced some areas such as Nordkapp Basin and Tromsø Basin in the Mesozoic to Cenozoic time (Faleide et al., 1984).

2.2 Structural elements

The Barents Sea consists of a complex of basins, platforms, structural highs and fault complexes (Figure 2.1). It is dominated by is NNE-SSW to NE-SW and NNE-SSW to NNW-

SSE trending structures (Gabrielsen et al., 1990). The western Barents Sea is has been overprinted by younger tectonic events. In contrast, most of the major structural trends in the eastern province may have been established by Late Paleozoic time because a calm period in terms of tectonic was in the eastern area of the Barents Sea since the end of the Carboniferous.

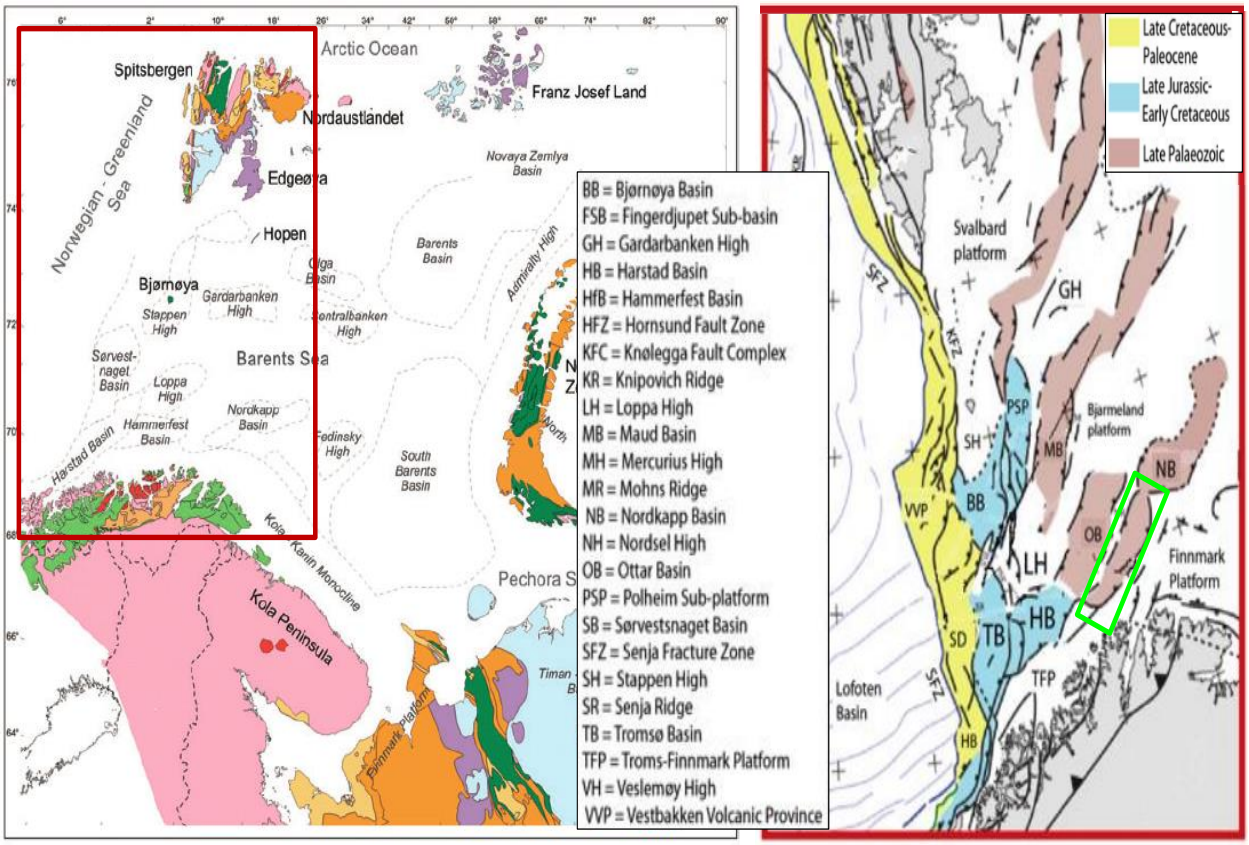

Figure 2. 1 Left: The main structure of the Barents Sea (Worsley et al. (2008)). Right: The main structural elements related to different rift phases affecting the SW Barents Sea with the study area marked by the green rectangle (modified from Faleide et al. (2010)).

2.3 General stratigraphy of the SW Barents Sea

In terms of sequence stratigraphy, tectonic activities, eustatic sea level changes and climatic conditions are the main factors controlling sedimentation and erosion in the sedimentary basins. Therefore, the Barents Sea's stratigraphy is characterized by lateral and vertical variations in thickness and facies of Paleozoic to Cenozoic sedimentary strata (Faleide et al., 2010).

The Upper Paleozoic strata is characterized by a variety of sediment type, from clastic sediments of the Lower Carboniferous succession to cyclical carbonate-rich sediment to massive limestone and evaporite of the lower part of the Upper Carboniferous to Permian succession. It includes a regional evaporate layer dated to the latest Carboniferous-earliest Permian in the SW Barents Sea (Faleide et al., 2010). In the late Early Permian, clastic sediment

started to dominate. The Mesozoic and the Cenozoic sediments consist of mainly clastic sediments. Some unconformities are observed. The Late Pliocene and Pleistocene glacial sediments lies on the top of the Mesozoic and Paleogene sediments. The uplift in the Late Cenozoic caused an erosion in a large scale which is the reason of 1000-1500 m of strata missing (Faleide et al., 2010).

The litho-stratigraphic column of the SW Barents Sea with important tectonic phases is presented in Figure 2.2.

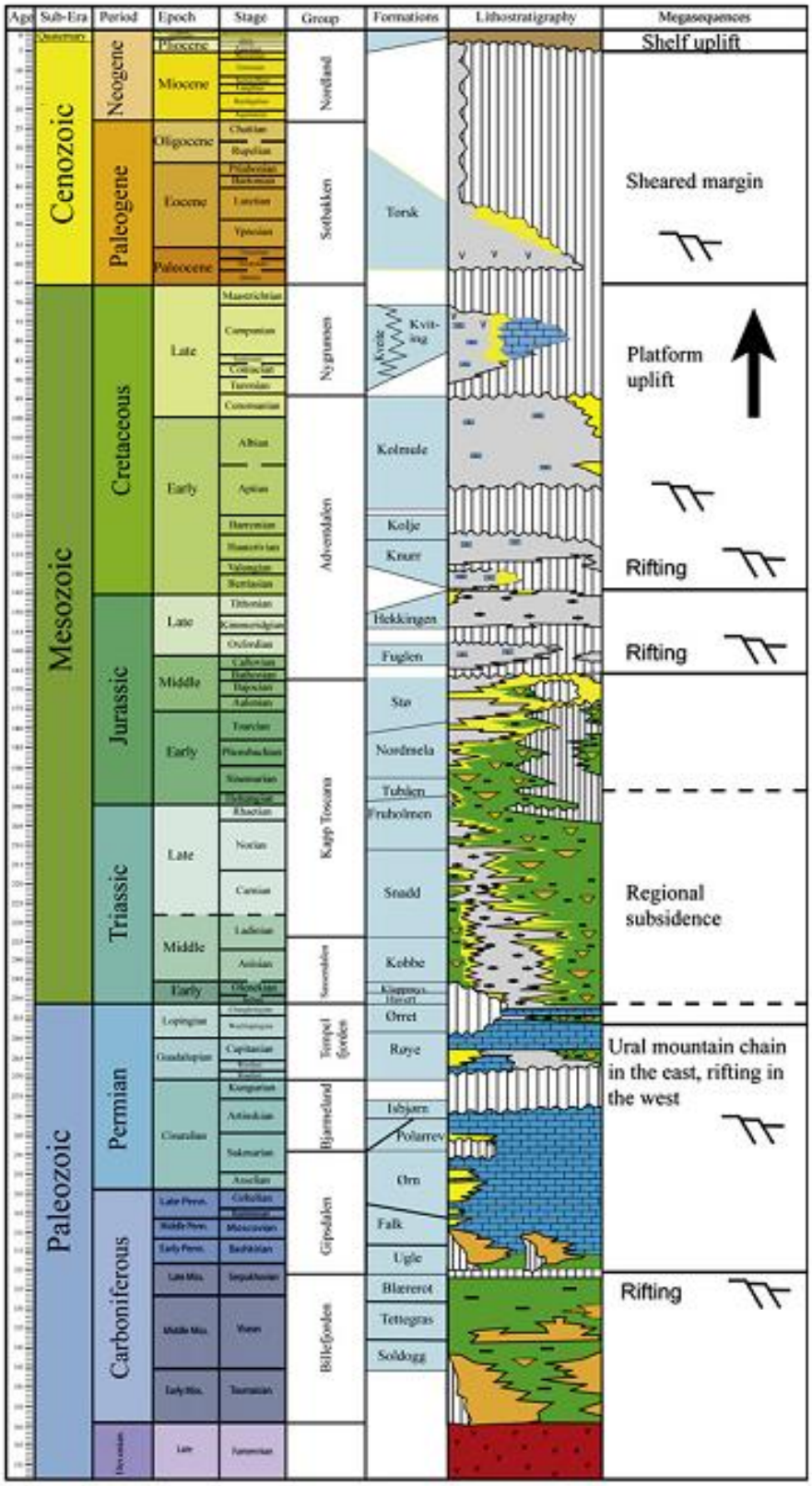

Figure 2. 2 Lithostratigraphic column in the SW Barents Sea with tectonic phases (Glørstad-Clark et al. (2010)).

2.4 The study area

The main focus of the thesis is salt in the southwestern part of the Nordkapp Basin located in the southwestern province of the Barents Sea. The study area and adjacent structural elements will be described generally.

2.4.1 The Nordkapp Basin

The Nordkapp Basin is situated in the southwestern province of the Barents Sea. It is a deep, narrow basin with a general ENE-WSW trend. It was formed during the Late Devonian to Early Carboniferous rift episode that occurred in the Barents Sea. The Nordkapp Basin is divided into three sub-basins: (1) the southwestern sub-basin trending NE-SW; the central sub-basin trending E-W; and (3) the northeastern sub-basin trending NE-SW. The extent of the northeastern sub-basin is wider and longer. The southwestern subbasin's margins are defined by the Nysleppen and Måsøy fault complexes (Figure 2.3).

The geological history of the basin shows the significant influence of salt diapirism (Gabrielsen et al., 1990). During Late Carboniferous - Early Permian, the existence of arid climate due to the change in latitude triggered the formation of large quantity of evaporate layer regionally in the SW Barents Sea, including the Nordkapp Basin (Faleide et al., 2010). After that, the increase of sediment loading and the active tectonics made the salt move upwards and create numerous salt structures with various geometries. The halokinesis in turn affected the basin development and sedimentation.

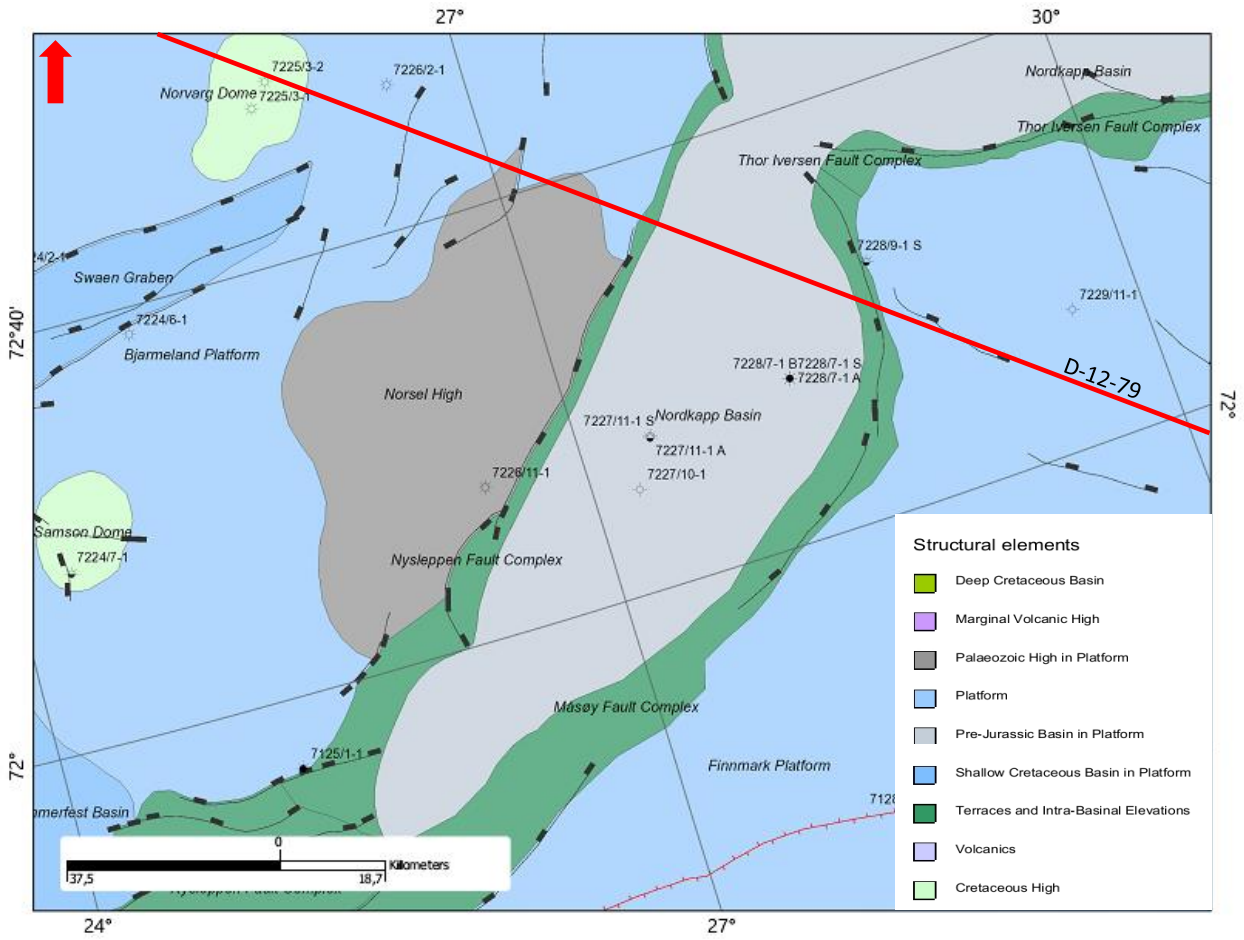

Figure 2. 3 The location and relation between the structural elements adjacent to the study area, the SW sub-basin of the Nordkapp Basin (NPD, 2016). The NW-SE oriented red line illustrates the location of the profile cross the study area, which is shown in Figure 2.4.

2.4.2 The Bjarmeland Platform

The Bjarmeland Platform is a tectonically stable area located to the northwest of the Nordkapp Basin (Figure 2.3). It was formed as a carbonate platform in Late Carboniferous to Permian time. After Late Paleozoic time, it shows little tectonic activity. Tertiary uplift causes the dipping to the south of sediments and the exposure of older sediments at the Base Quaternary Unconformity in the Bjarmeland Platform (Gabrielsen et al., 1990).

2.4.3 The Norsel High

The Norsel High is a NE-SW trending structure situated on the Bjarmeland Platform (Figure 2.3). The Norsel High was formed during the tectonic activity in Early Carboniferous. It remained as a high until Middle Triassic (Gabrielsen et al., 1990).

2.4.4 The Nysleppen Fault Complex

The Nysleppen Fault Complex is situated at the boundary between the Bjarmeland Platform/Norsel High to the northwest and the Nordkapp Basin to the southeast (Figure 2.3). It consists of several fault sets. Faults in each set are arranged in an en échelon style. Carboniferous is inferred to be the time of the main fault activity (Gabrielsen et al., 1990). Faults were reactivated in Late Jurassic to Early Cretaceous and Tertiary times. The complexity of the Nysleppen Fault Complex increases. The Nysleppen Fault Complex is associated with large salt pillows.

2.4.5 The Måsøy Fault Complex

The Måsøy Fault Complex separates the Finnmark Platform and the southwestern part of the Nordkapp Basin (Figure 2.3). It is an extensional structure. It is dominated by NE-SW trending faults arranged in an en échelon fashion. The main fault activity is suggested to be of Carboniferous age (Gabrielsen et al., 1990). During the Late Jurassic to Early Cretaceous and Tertiary tectonic episodes, Carboniferous faults were reactivated due to extension (Talbot et al., 1993). The Måsøy Fault Complex along the Nordkapp Basin's margin is associated with salt pillows (Gabrielsen et al., 1990).

2.4.6 The Finnmark Platform

The southern boundary of the Finnmark Platform is the Norwegian mainland. Its northwestern part is adjacent to the Måsøy Fault Complex and the Nordkapp Basin (Figure 2.3). It has been a stable area since the Late Palaeozoic. Before that time, possibly pre-Carboniferous time, it has a pronounced rift topography with NE-SW trending faults. In Tertiary, in contrast to sediments in the Bjarmeland Platform, sediments here dip to the north due to the uplift (Gabrielsen et al., 1990).

Figure 2.4 represents a NW-SE oriented profile showing the change in structural style as well as the litho-stratigraphy cross the study area.

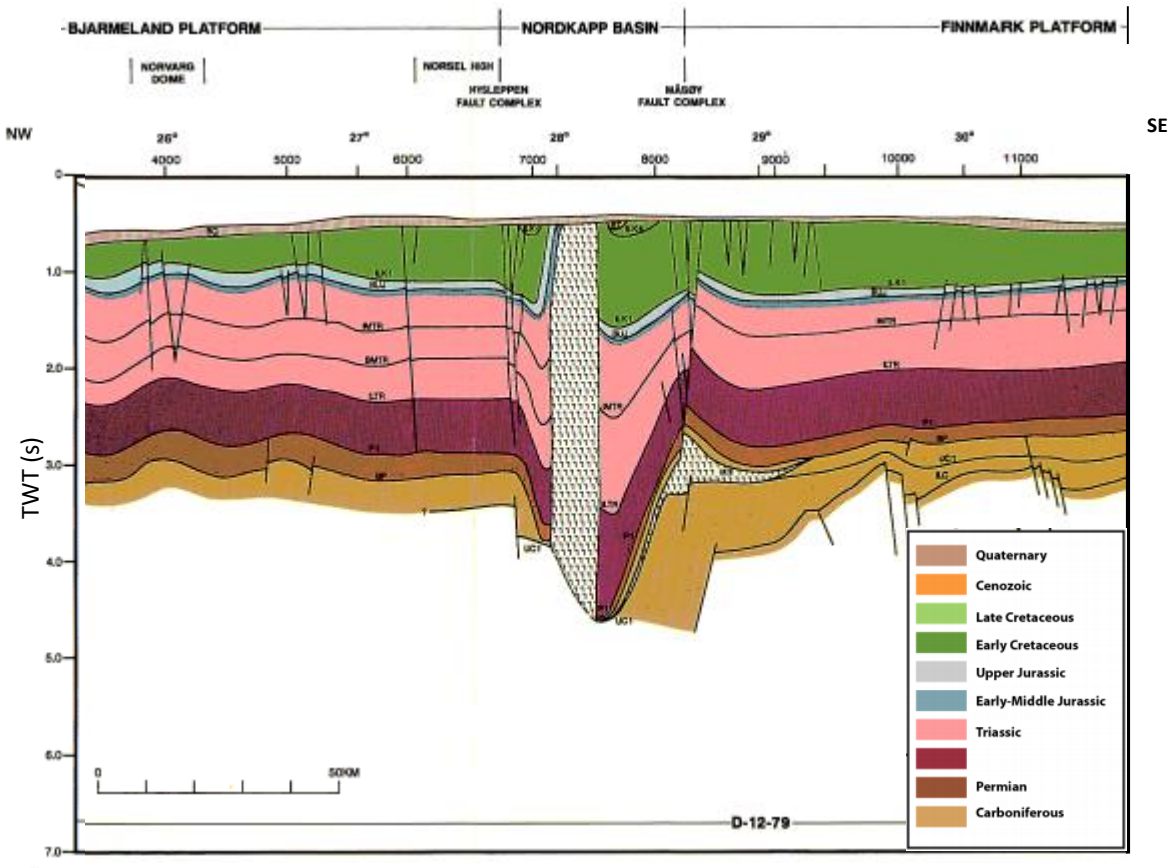

Figure 2. 4 Profile showing Bjarmeland Platform in the northwest, Finnmark Platform in the southeast and the Nordkapp Basin in the center. Norvarg Dome and Norsel High are parts of Bjarmeland Platform. Nysleppen and Måsøy Fault Complexes are the transition between the platforms and the basin. Interpreted lithology is given by colored intervals (modified from (Gabrielsen et al., 1990).

3 PROPERTIES AND MOBILIZATION OF EVAPORITES

3.1 Evaporites

Evaporites are chemical sediments deposited in the basins where evaporation exceeds influx (Figure 3.1). Hence, evaporite basins usually develop in semi-arid and arid regions of the globe (Jenyon, 1986).

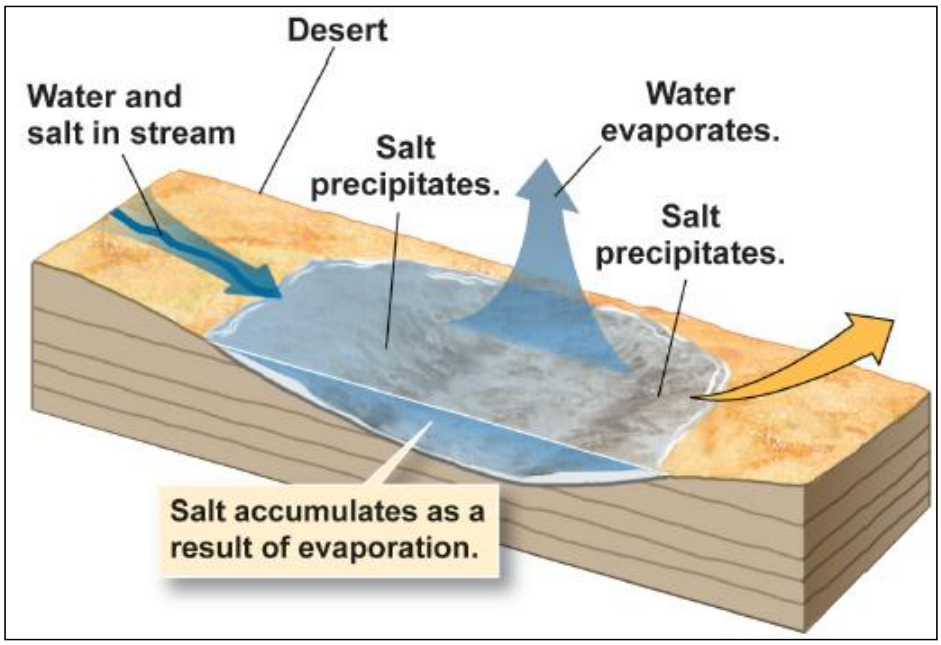

Figure 3. 1 Evaporties accumulates as a result of evaporation (Marshak et al., 2001).

Various types of mineral precipitate when decreasing water volume (Figure 3.2). Two common evaporite minerals, halite (NaCl) (rock salt) and gypsum ($CaSO_4.2H_2O$), precipitate when the water concentrates to about 10% and 20% of its original volume.

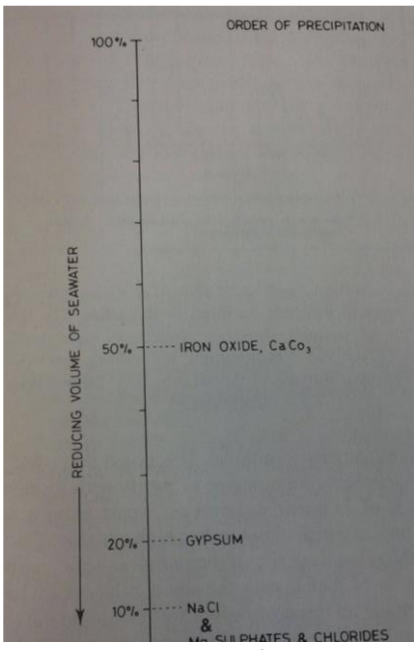

Figure 3. 2 The order of precipitation of minerals from sea water which is evaporated (Jenyon, 1986).

3.2 Characteristics of salt rock

Salt rocks are formed mainly from the mineral halite whose density of approximately 2.17 g/cm^3 is invariant with depth. Differently from other sedimentary rocks, salt shows no effects of compaction with increasing depth of burial. Hence, salt layers become buoyant and gravitationally unstable when buried to depths where the bulk density of the overburden is larger than the salt density (Figure 3.3). Consequently,

upward movement of salt takes place (Jenyon, 1986). Moreover, salt is viscous and impermeable. In addition, salt has high heat conductivity. Those properties are considerable in terms of petroleum exploration field. Salt's viscous behaviour and impermeability make it efficient top and side seals (Fossen, 2010). Besides, the presence of salt affects the heat flow of a basin. The underlying sediments get cooled. For this reason, source rock maturation may happen at greater depths in comparison with basins having the normal thermal gradient. It influences the depth of oil and gas windows (Fossen, 2010).

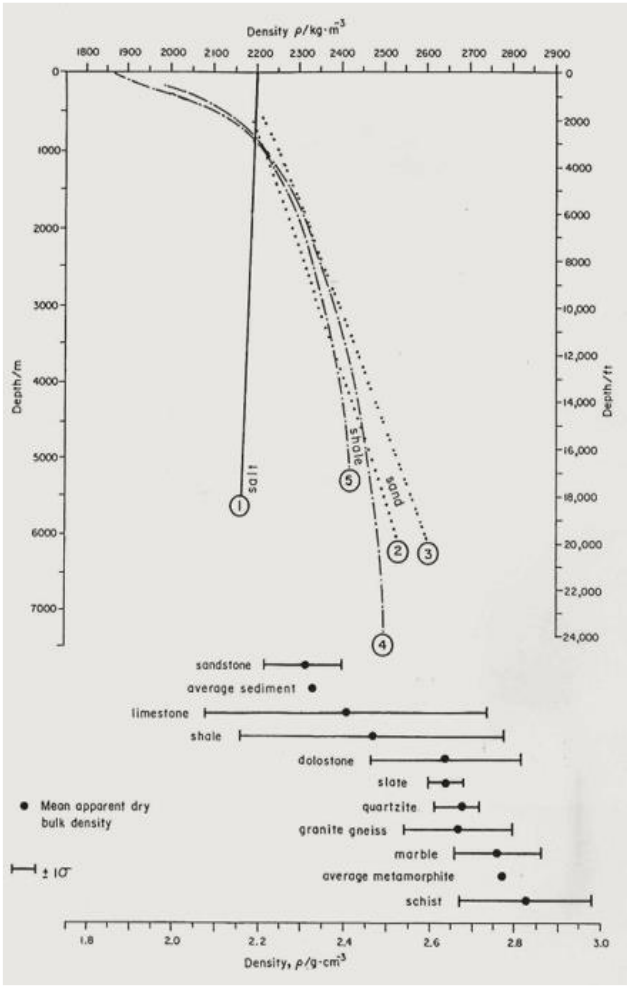

Figure 3. 3 Curves of constant density of salt in comparison with density change of other types of sediment following burial depth (Jenyon, 1986).

However, the unique properties of salt make mapping of salt structures and understanding salt processes a challenge. Firstly, high velocity and low density of salt as compared to those of surrounding sedimentary strata produce large reflection coefficients which create strong seismic reflection representing the salt-sediment boundaries. Seismic velocity of salt is 4500 m/s. Furthermore, the velocity differences cause positive/negative velocity anomalies or "pull-up" and "pull-down" features in seismic section which are different from real-earth image.

Nevertheless, the energy after travelling through salt is much attenuated. Thus, the sediment layers beneath salt bodies are poorly imaged in seismic section. Secondly, salt structures usually have vertical flanks due to the upward movement of salt. It is hard to get a clear image of the salt flanks and sediments nearby. These bring huge uncertainty and risk for drilling salt-related traps in the petroleum exploration.

3.3 Halokinesis

Halokinetic models have been used to describe salt movement process in relationship to the tectonic styles and sedimentation to explain the geometry of salt structures and halokinetic sequences such as Trusheim (1960); Hudec et al. (2007) and Fossen (2010).

3.3.1 Main causes of salt movement

Previous models demonstrate that upward movement of salt is triggered by differential loading, thermal convective or displacement loading (Trusheim (1960); Fossen (2010); Woodbury et al. (1980)) (Figure 3.4). A tectonic event can induce and support the salt movement. Faulting during extension or compression can help create the movement way. Moreover, an extensional event provide space for salt and reduce the strength of the overburden (Fossen, 2010). Whereas, during a contractional event, a compress force is put on the incompressible salt to shorten it and force it move upward. The salt is squeezed.

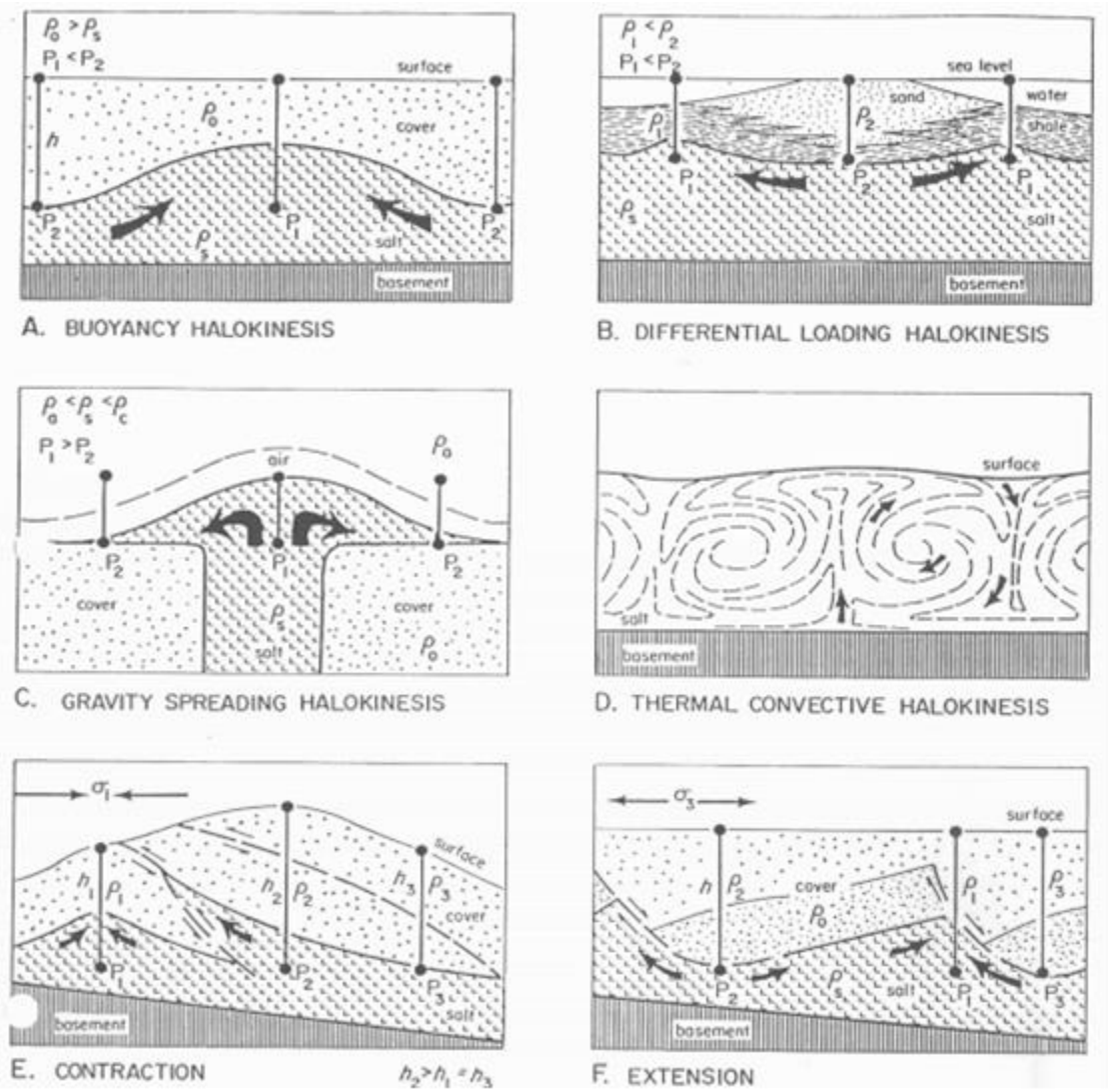

Figure 3. 4 Triggering mechanisms of salt movement (Woodbury et al., 1980).

3.3.2 Stages of salt movement and effect on sediment

The first stage of salt movement is called doming to create salt pillow structures (Figure 3.5.1). The overburden are rotated upwards and eroded. The depletion of the mother salt layer occurs. Fossen (2010) called it downbuilding process. Therefore, the withdrawal of salt creates small mini-basins or depo-centers close to the positive salt structure. They are called primary rim synclines. The thickness of sediment deposited in the mini-basins decreases towards the salt pillow.

The salt keep moving upwards until it reaches the sedimentary level (Figure 3.5.2). The differential loading of overburden induces the salt to continue moving from the salt source layer towards the diapir and flow upwards. Second rim synclines are formed and filled by growth strata (Figure 3.5.3).

When the total depletion of the salt mother layer happens or the diapir does not connect to the salt mother layer, the upward movement of salt will stop due to the lack of salt supply. After that, it is buried and covered by sediments (Figure 3.5.4).

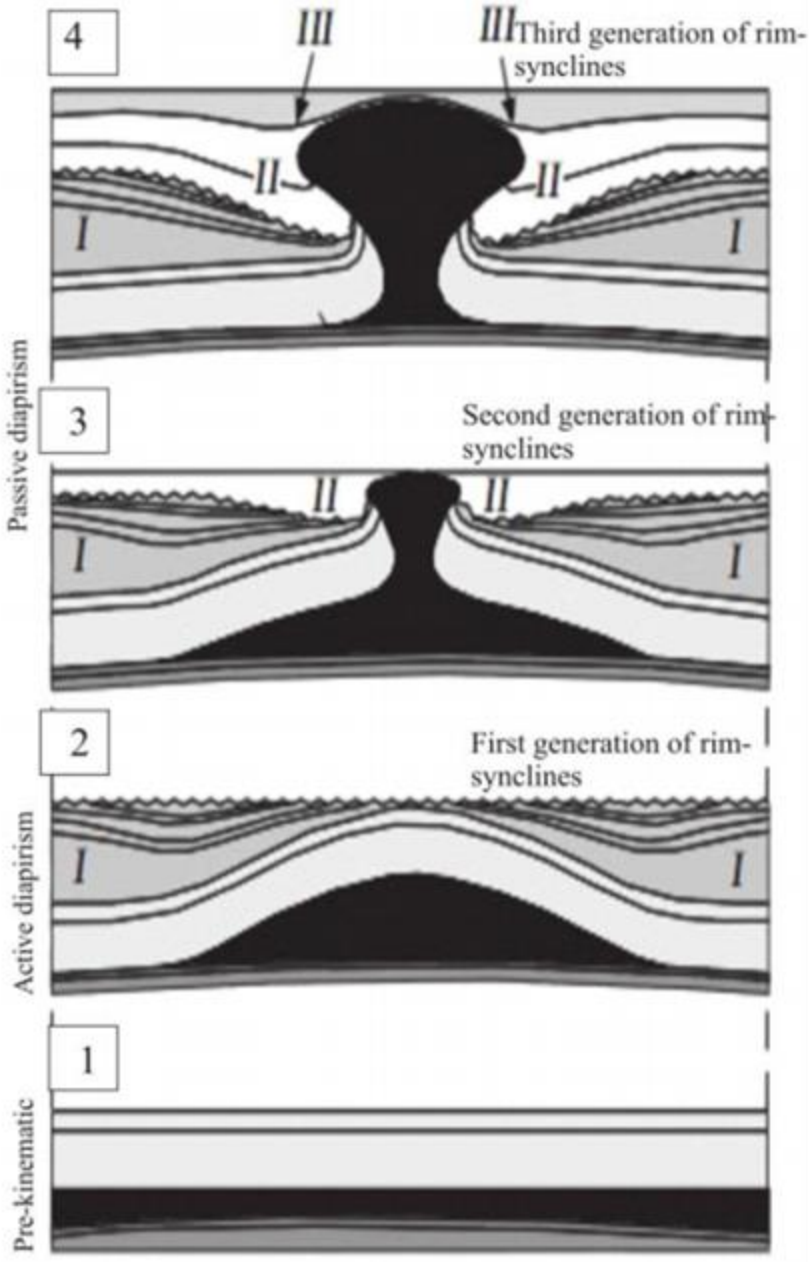

Figure 3. 5 Stages of salt movement. Active diapirism and passive diapirism (Trusheim, 1960).

McGuinness et al. (1993) and Giles et al. (2002) studied the relationship of the net sedimentation rate and the net salt supply (Figure 3.6 - 3.7). The general ideas are:

- When the rate of sedimentation is smaller than the rate of salt growth, salt diapir has a widening shape with the off-stepping halokinetic sequence stacking (Figure 3.6.a). The

sedimentary sequence deposited at the same time as the salt movement develops the overturned beds with the dip $\alpha > 90^o$ (Figure 3.7).

- When the rate of sedimentation is equal to the rate of salt growth, the salt structures develop vertical flank with the dip α of 90^o (Figure 3.6). Halokinetic sequences stack vertically (Figure 3.7b).
- When the rate of sedimentation is larger than the rate of salt growth, the dip of salt-sediment interface α is less than 90^o (Figure 3.6). Onstepping halokinetic sequence stacking is observed (Figure 3.7c).

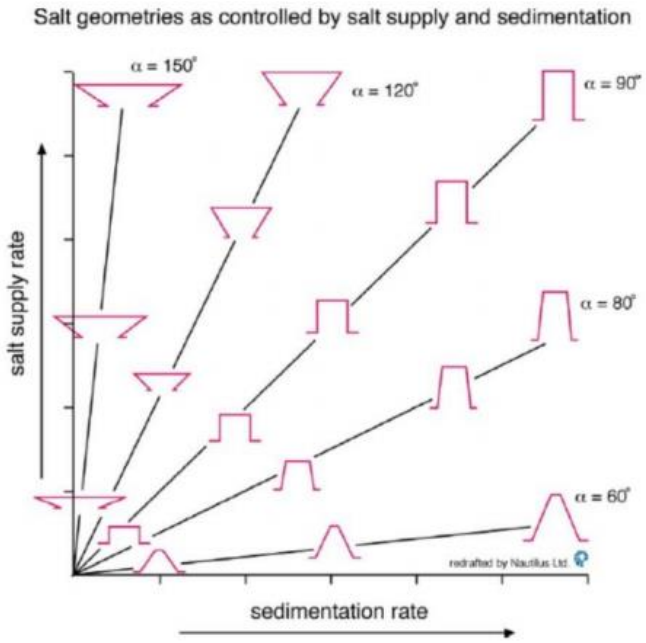

Figure 3. 6 The relationship of sedimentation rate and salt growth rate affect the dip of salt-sediment interface, α (McGuinness et al., 1993).

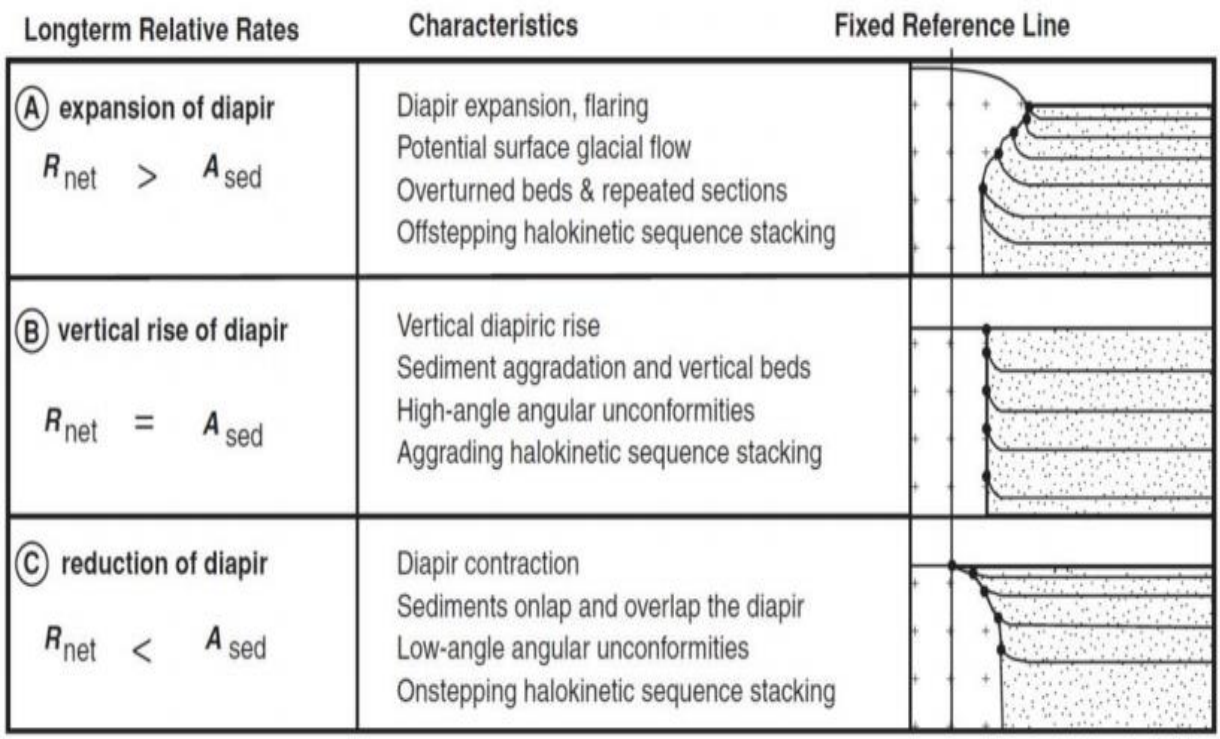

Figure 3. 7 The illustration for the relationship of the net sedimentation rate and salt supply rate influencing the shape of salt structures and the contact between salt and sediment (Giles et al., 2002).

3.4 Classification of salt structures

The geometry of salt structures depends on many factors such as the salt mother layer thickness, the properties of overburden, the sedimentation or erosion rate and tectonic regime (Fossen, 2010). Hence, different types of salt structures develop with variation in size, shape and frequency (Figure 3.8).

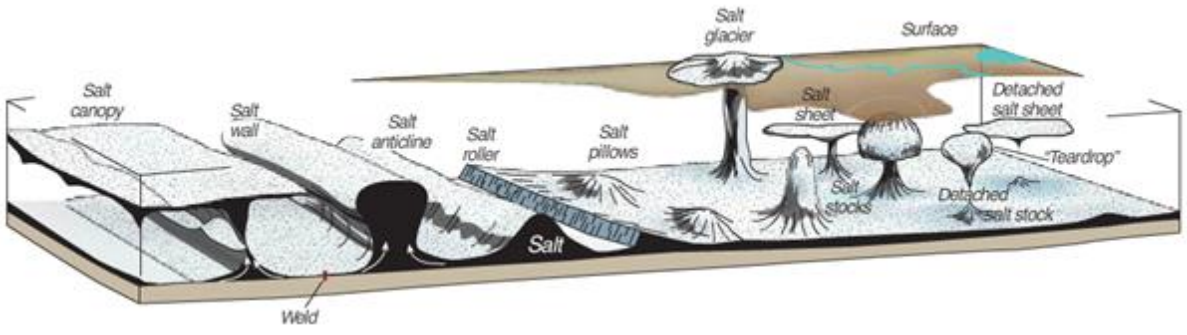

Figure 3. 8 The diagram shows the major types of salt structure. The structural maturity and size increases toward the composite, coalesced structures (Fossen, 2010).

4 DATABASE AND SEISMIC INTERPRETATION RESULTS

4.1 Database

The database consists of sixty-nine 2D seismic lines and wells located in the study area (Figure 4.1). The dataset was provided by TGS/Fugro and the Norwegian Petroleum Directorate (NPD).

The seismic lines are oriented WNW-ESE, NNW-SSE and SW-NE. They are from different surveys. The distance between two adjacent lines varies. It leads to the difference in seismic coverage throughout the area. Moreover, the quality and the depth penetration are not the same in all 2D surveys.

Two wells were used for the stratigraphic calibration and well to seismic tie. Well 7226/11-1 is located on the Norsel High in the southeastern part of the Bjarmeland Platform. It lies close to the northwestern margin of the southwestern part of the Nordkapp Basin. In contrast, Well 7228/9-1 is located on the western margin of the Finnmark Platform, close to the Måsøy Fault Complex. The general information of wells has been taken from the FactPage of the Norwegian Petroleum Directorate (NPD) (Table 4.1).

Additional data, which are used for detailed interpretation of salt structures, consists of time-slices from two pseudo-3D seismic cube and filtered gravity anomalies from Courtesy of TGS.

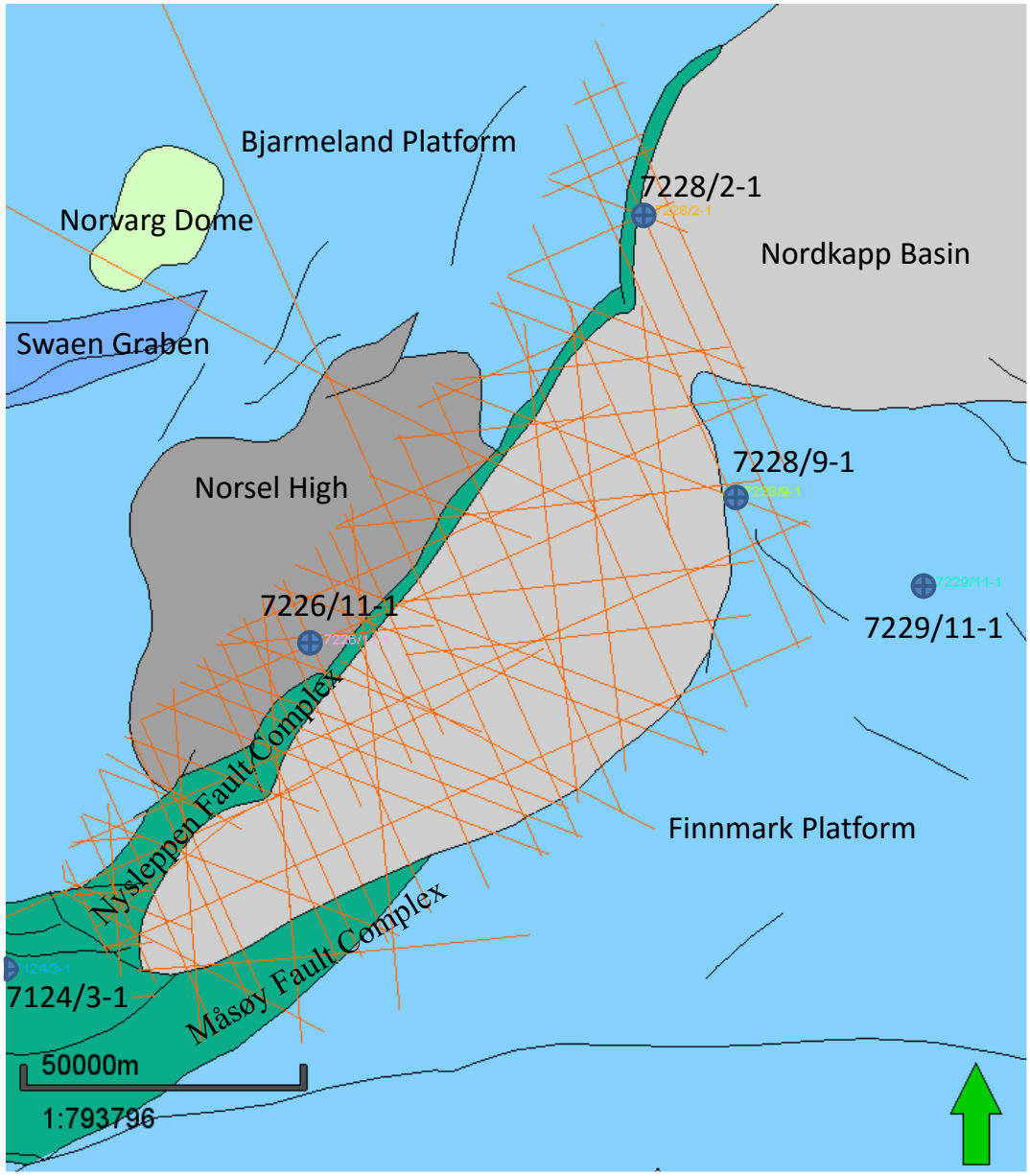

Figure 4. 1 Map of the 2D seismic grid and well location used in the study.

Wellbore name	7226/11-1	7228/9-1
NS degrees	72° 14' 18.16'' N	72° 23' 48.36'' N
EW degrees	26° 28' 44.78'' E	28° 43' 8.67'' E
NS UTM (m)	8015817.52	8034238.91
EW UTM (m)	482263.45	558023.28
UTM Zone	35	35
Seismic Location	D-14-84A SP. 1349/N-1-86 SP. 5667	SH 87 - 178 SP 722
Main Area	Barents Sea	Barents Sea
Drilling Operator	Den norske stats oljeselskap a.s	Norsk Hydro Produksjon AS
Drilling Days	173	137
Completion Date	11.04.1990	07.05.1990
Type	Exploration	Exploration
Status	P & A	P & A
Discovery Wellbore	Yes (Gas)	No
Kelly Bushing Elevation (m)	23.0	23.5
Water Depth m)	237.5	278.0
Total Depth (MD) (mRKB)	5200.0	4600.0
Oldest penetrated age	Pre-Devonian	Early Permian
Oldest penetrated formation	Basement	ØRN Formation

Table 4. 1 General information of the wells used for seismic to well correlation in the study. See Figure 4.2 for location of wells (NPD, 2016).

4.2 Interpretation software

Petrel version 2015 software has been utilized for seismic interpretation during thesis work. It was provided by Schlumberger. A project in Petrel 2015 was created with the 2D seismic data and well data.

4.3 Selected seismic reflections

The generalized workflow of the study is shown in Figure 4.2. A general overview of the data has been carried out to familiarize with the structural elements and regional geological settings of the study area. Afterwards, two good and regional, continuous reflections were selected and mapped throughout the study area. They are Base Cretaceous and Near Top Permian. The interpretation of faults, especially boundary faults was also conducted. The next step was

detailed interpretation of the main sequences by using well data, mainly well tops to correlate to the seismic reflections, for better understanding of the stratigraphic evolution. Six main reflections calibrated to six well formations were identified and interpreted (Table 4.2).

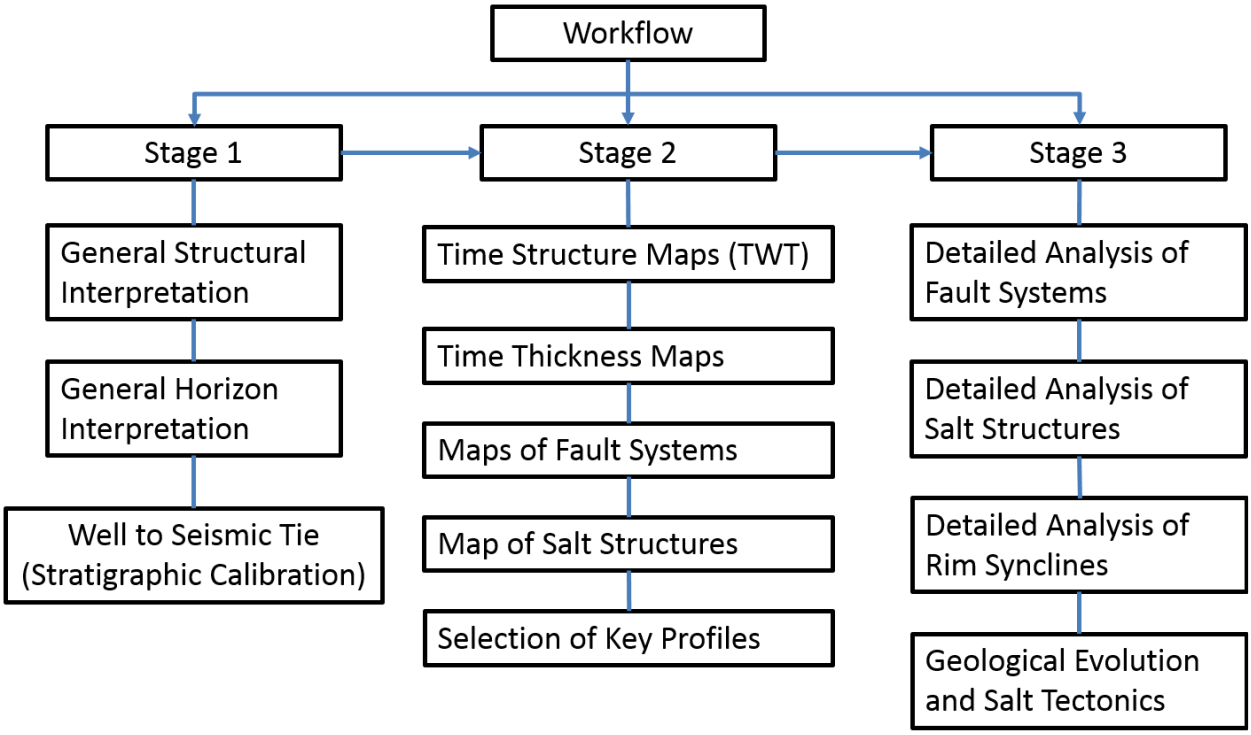

Figure 4. 2 Generalized workflow of the study.

Formation	Age	Color
Hekkingen Formation	Base Cretaceous	
Fuglen Formation	Middle Jurassic	
Kobbe Formation	Anisian - Intra Middle Triassic	
Klappmys Formation	Olenekian – Early Triassic	
Havert Formation	Induan – Early Triassic	
Røye Formation	Near Top Permian	

Table 4. 2 Colored codes for the interpreted horizons

4.4 Key Profiles

Four 2D lines were carefully selected for illustrating the structural differences from southwest to northeast of the study area. All the key lines cut through parts of the Bjarmeland Platform

and Nysleppen Fault Complex in the northwest, crossing the southwestern part of the Nordkapp Basin in the center and the Måsøy Fault Complex and parts of the Finnmark Platform in the southeast.

Figure 4.3 shows the location of the four key lines with the main faults and salt structures in the study area. The construction of maps in Figure 4.3 will be presented later, in the sub-chapter 4.5.4.

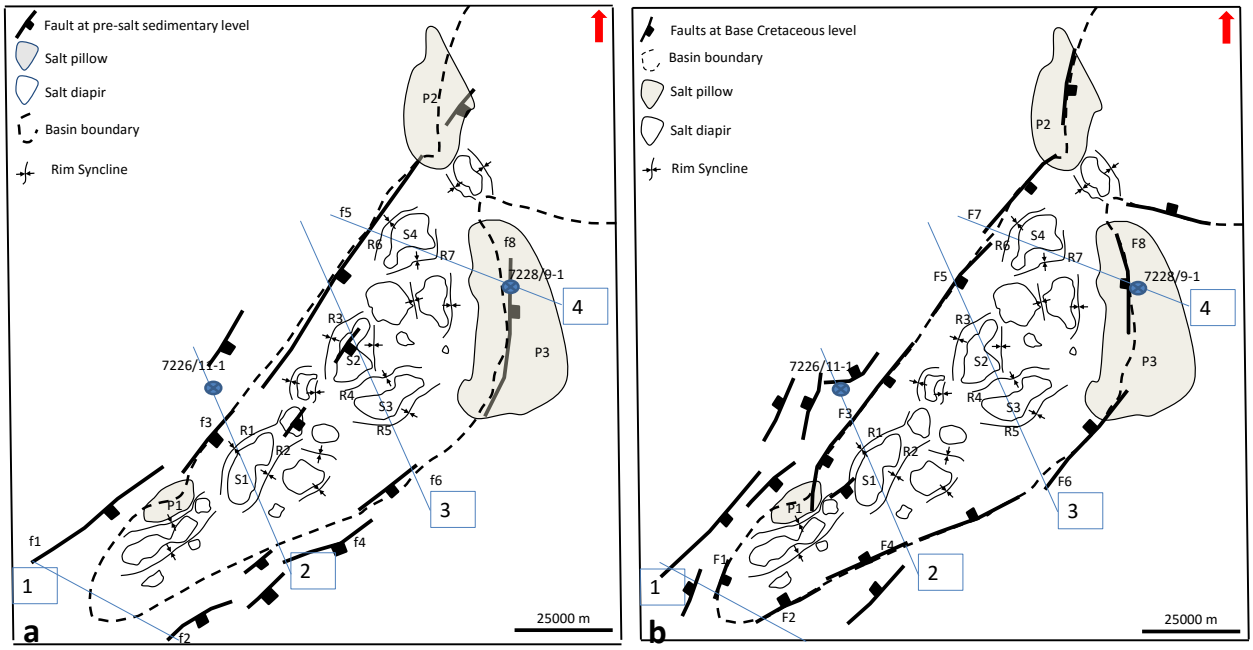

Figure 4. 1 The maps showing main faults and salt structures with the location of four key profiles. Left: Faults at pre-salt sedimentary level. Right: Faults at Base Cretaceous level.

4.5 Description of maps and key profiles

4.5.1 Overall observation from maps of fault systems

The Nysleppen Fault Complex defines the northwestern boundary of the basin. The map (Figure 3.3) shows the general trend of it is NE-SW. At the Norsel High, several fault segments with a NNE-SSW-strike occur. As defined at the pre-salt level, it consists of normal faults dipping towards the SE (Figure 4.3a). However, at the level of the Base Cretaceous, the Nysleppen Fault Complex contains two series of faults with opposite dip-direction (Figure 4.3b). A relay ramp is observed between fault segments F5 and F7 at the Base Cretaceous level. The fault zone is associated with salt pillows (P1 and P2) (Figure 4.3).

The Måsøy Fault Complex defines the southeastern margin of the basin. The main trend of faults is ENE-WSW (Figure 4.3). At the pre-salt level, the boundary fault is a normal fault

dipping SE (Figure 4.3a). In contrast, at the level of Base Cretaceous, faults of the Måsøy Fault Complex have different dip-direction. They are normal faults dipping NW. The fault zone at the Base Cretaceous is narrower than that at the pre-salt level. In addition, the fault zone is also associated with the salt pillow P3.

4.5.2 Description of the key profiles

Key profile 1

Key profile 1 is the southernmost of the key-lines. The orientation of the line is NW-SE and is perpendicular to the main trend of faults (Figure 4.3). It goes through the part of the southwestern sub-basin of the Nordkapp Basin which is not affected by diapirs (Figure 4.4).

Fault f1 belongs to the Nysleppen Fault Complex. Its strike is NE-SW (Figure 4.3). Fault f1 is a normal fault dipping towards the SE. It is characterized by a planar geometry. Fault f1 shows a large vertical separation of about 1.50 s TWT (two-way time). The fault was active at pre-salt level (Late Paleozoic), below the refection B. Variation in the thickness of sediments across the fault f1 is clear. The Late Paleozoic package on the footwall has less thickness as compared to that on the hanging wall, 0.5 and 2.0 s, respectively (Figure 4.4a). Fault f2 of the Måsøy Fault Complex has similar characteristics to those of fault f1. However, the vertical separation of f2 is approximately 0.25 s, which is much smaller than that of f1. Faults f1 and f2 represent the major half graben structure in the area at Late Paleozoic level with the large subsidence along the northwestern margin where f1 is the bounding fault (Figure 4.4a).

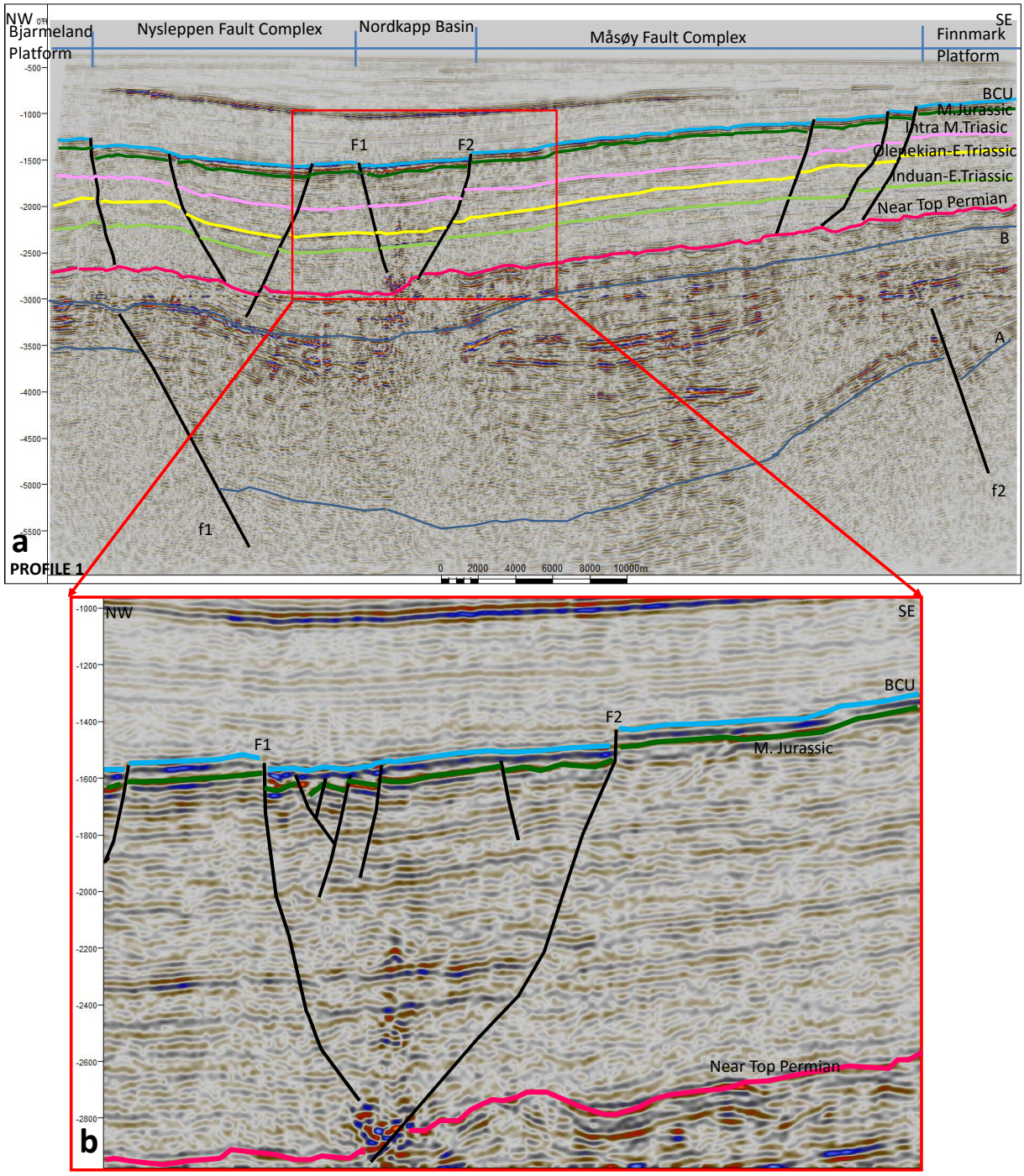

Figure 4. 2 (a) Profile 1 illustrating the structural elements of the southwesternmost part of the study area which is not affected by diapirsim. Reflections A and B are interpreted in this seismic line for detailed interpretation of timing of faults at deeper level. (b) The zoomed part of (a) in the Nordkapp Basin represented by red square.

Fault F1 of the Nysleppen Fault Complex is the bounding fault in the northwestern margin of the Nordkapp Basin. It strikes NNE-SSW (Figure 4.3). F1 is a normal fault with the dipping to the SE. It has a listric geometry. Its vertical separation is around 0.04 s. The sediment package between the Middle Jurassic and BCU (Base Cretaceous Unconformity) shows variation in the thickness across the fault (Figure 4.4b). The Jurassic sediment has a wedge

shape on the hanging wall of the fault. The sediment below and above this interval has a relatively constant thickness across the fault. Those indicate the activation of fault F1 during deposition of the Jurassic sediment. Fault F2 is similar to F1. However, its strike is more ENE-WSW and it has the opposite dip-direction. While F1 ends in the Triassic interval, F2 cut deeper, through the Near Top Permian reflection.

An overall observation is that the fault system at Base Cretaceous level is more complicated than that at Late Paleozoic level. It consists of several normal faults with different orientation, dip and geometry. It creates the graben and horst structures (Figure 4.4a). In the Nordkapp Basin, it consists of antithetic and synthetic faults along with the master faults, F1 and F2 (Figure 4.4b). While the Nysleppen Complex Fault is made of two fault series with opposite dips, the Måsøy Fault Complex is composed of the fault series with the dip-direction towards the NW. Moreover, most of the splaying, curved faults at Base Cretaceous level cut down the section and end at Near Top Permian (Figure 4.4a). In addition, the throw of faults at the Base Cretaceous is much smaller than that of faults at pre-salt level.

Key profile 2

Profile 2 is a NNW-SSE-oriented seismic line. It goes straight through the well 7226/11-1 located on the Bjarmeland Platform. The basin is affected by one large salt diapir (Figure 4.5).

Fault f3 of the Nysleppen Fault Complex strikes NE-SW with SSE dip (Figure 4.3). It is a normal fault with a planar configuration (Figure 4.5a). Fault f3 is similar to fault f1 in Key Profile 1 (Figure 4.4a). However, it shows a larger vertical displacement of 2.25 s at pre-salt (Late Paleozoic) level (horizon A) than f1). Fault f4 of the Måsøy Fault Complex has the same dip-orientation, strike and geometry as fault f2 in Key Profile 1 (Figure 4.4a). As compared to f2, the vertical separation of f4 at Late Paleozoic level is larger, approximately 0.5 s.

Fault F3 belongs to the Nysleppen Fault Complex. Its general trend is NE-SW. The southwestern part of F3 with an N-S strike has a curved shape in the horizontal dimension (Figure 4.3). The curved part of F3 is at the position of a salt pillow in the map. F3 is a normal fault dipping towards SSE. It has a listric configuration with a throw of 0.1 s. It cut through the stratigraphic succession from Near Top Permian to Base Cretaceous. It stops right at the Near Top Permian reflection (Figure 4.5a). A variation in sediment thickness of the package from Middle Jurassic to Base Cretaceous across the fault F3 is observed. Besides the opposite dip-orientation, F4 of the Måsøy Fault Complex has similar characters to F3.

A salt structure named S1 is situated in the center of the basin. S1 has an upward-widening shape. Its diameter is around 10 km. Its extent is approximately 20 km in length. Its strike is NNE-SSW (Figure 3.3). The salt wall intruded to the near sea floor. The salt flanks themselves are difficult to map accurately because salt structures usually have vertical flanks due to the upward movement. It is hardly to trace the base of salt structure because of poor image beneath the salt. The seismic energy after travelling through salt is much attenuated. There is evidence of erosion at the top of the salt wall.

Generally, the sediments from Near Top Permian to Base Cretaceous have a discordant contact with salt wall. They terminate and onlap to the salt flanks. The sediments are draped upward (Figure 4.5a). Moreover, the continuity and the amplitude of reflections within the sequence increase upwards.

At the upper boundary of the Induan (Early Triassic) sequence, truncation is present in areas adjacent to the salt structure S1 (Figure 4.5b). The Olenekian (Early Triassic) package consists of divergent reflections. The sequence has a large thickness variation. The sequence is significantly thicker towards the salt wall. The intensity of the drape folding increase upwards the sequence, from slight folding layers at the base to overturned layers at the top. Aggradation halokinetic sequence stacking is present.

The sequence between Olenekian (Early Triassic) and Intra Late Triassic shows smaller thickness variations in comparison to the Olenekian (Early Triassic) sequence. The layers are affected by a strong drape folding. Overturned truncations at the flanks of the salt wall are shown. Off-stepping halokinetic sequence stacking is present.

The Intra Late Triassic – Middle Jurassic sequence also has small variation in thickness. Strong drape folds affect the sediment. The halokinetic sequence stacking is similar to that in the Olenekian (Early Triassic) – Intra Late Triassic sequence. The sediments of the upper part lie nearly flat. The Jurassic sequence has a relatively constant thickness, and it is draped on the upper boundary of the salt structure.

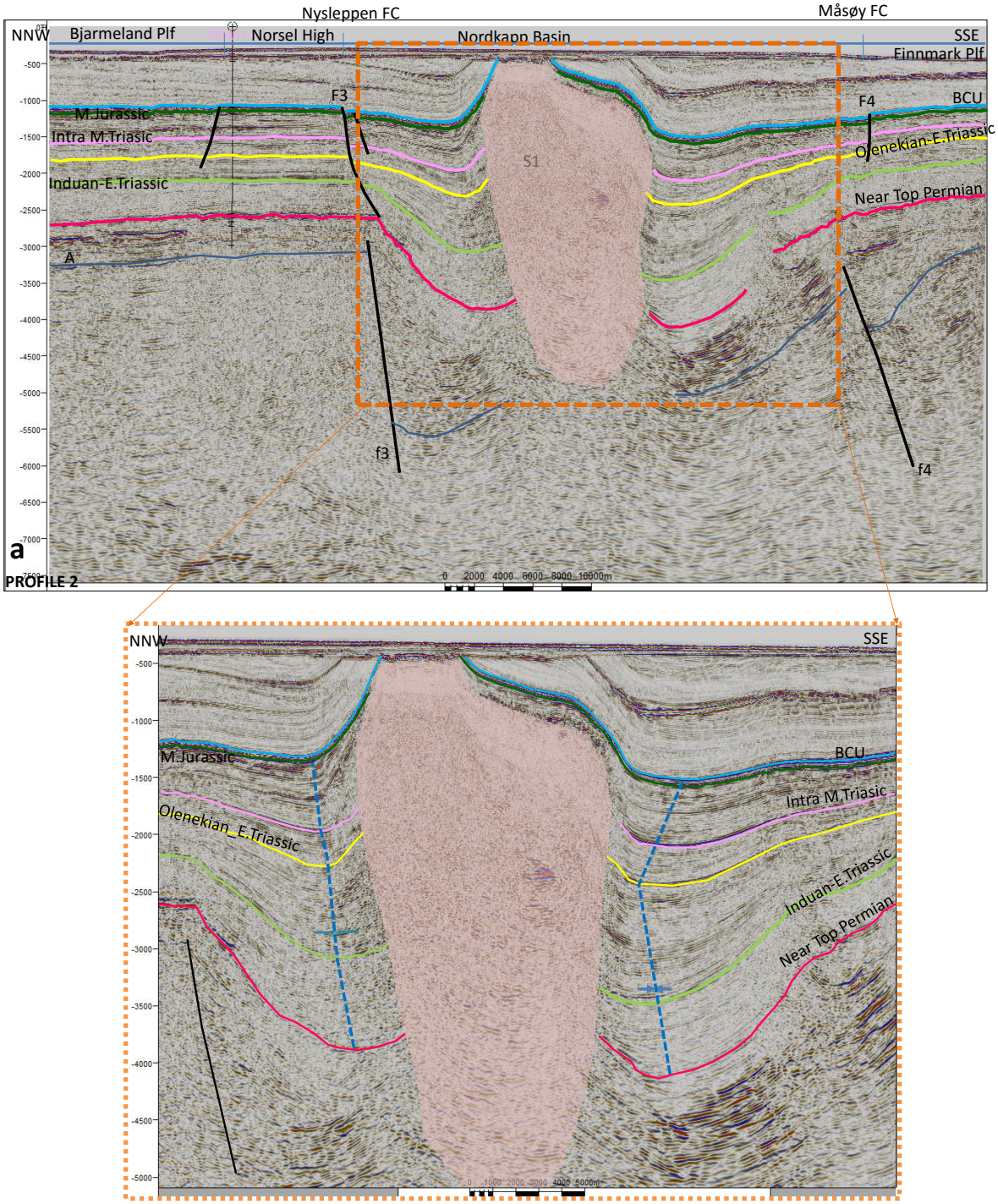

Figure 4. 3 Key Profile 2 across the well 7226/11-1 located on the Bjarmeland platform. The basin is affected by one large diapir. Diapir is colored by light pink. Rim syncline axis is marked by dotted blue line.

Key profile 3

Profile 3 transects the central part of the Nordkapp Basin which is strongly affected by salt diapirism (Figure 4.6).

Fault f5 of the Nysleppen Fault Complex strikes NE-SW with SSE dip (Figure 4.3). Fault f5 is similar to fault f1 in Key Profile 1 and f3 in Key Profile 2 (Figures 4.4 and 4.5). It is normal

and planar. It shows a vertical displacement of 2.0 s at pre-salt (Late Paleozoic) level. Fault f6 of the Måsøy Fault Complex has the same dip-orientation, strike and geometry as faults f2 and f4 in previous profile (Figure 4.3).

Fault F5 of the Nysleppen Fault Complex is the bounding fault segment in the northwestern margin of the basin. It strikes NE-SW (Figure 4.3). F5 is a normal fault with the dip-direction being SSE. It has a listric geometry. Its vertical separation is around 0.12 s (Figure 4.6). Fault F6 is similar to F5. However, it has the opposite dip-direction. F5 and F6 cut through the sequence from Near Top Permian to Base Cretaceous. They splay and end right above the Near Top Permian reflection (Figure 4.6).

Two separate salt walls are observed. Differently from S1 and S2, S3 has a more or less vertical shape. S2 is 7.5 km in width and 15 km in length while S3's dimensions are 5 km and 15 km. The strike of S2 is similar to that of S1, whereas, the strike of S3 is more ENE-WSW (Figure 4.3). The discordant contact, the evidence of erosion and flaps (bent layers) developing along its upper margins are also found. However, the erosional part of the upper part of the diapir S3 is covered by Quaternary horizontal strata (Figure 4.6). Moreover, there are evidence of the residual salt which is characterized by strong reflections at the base and the top.

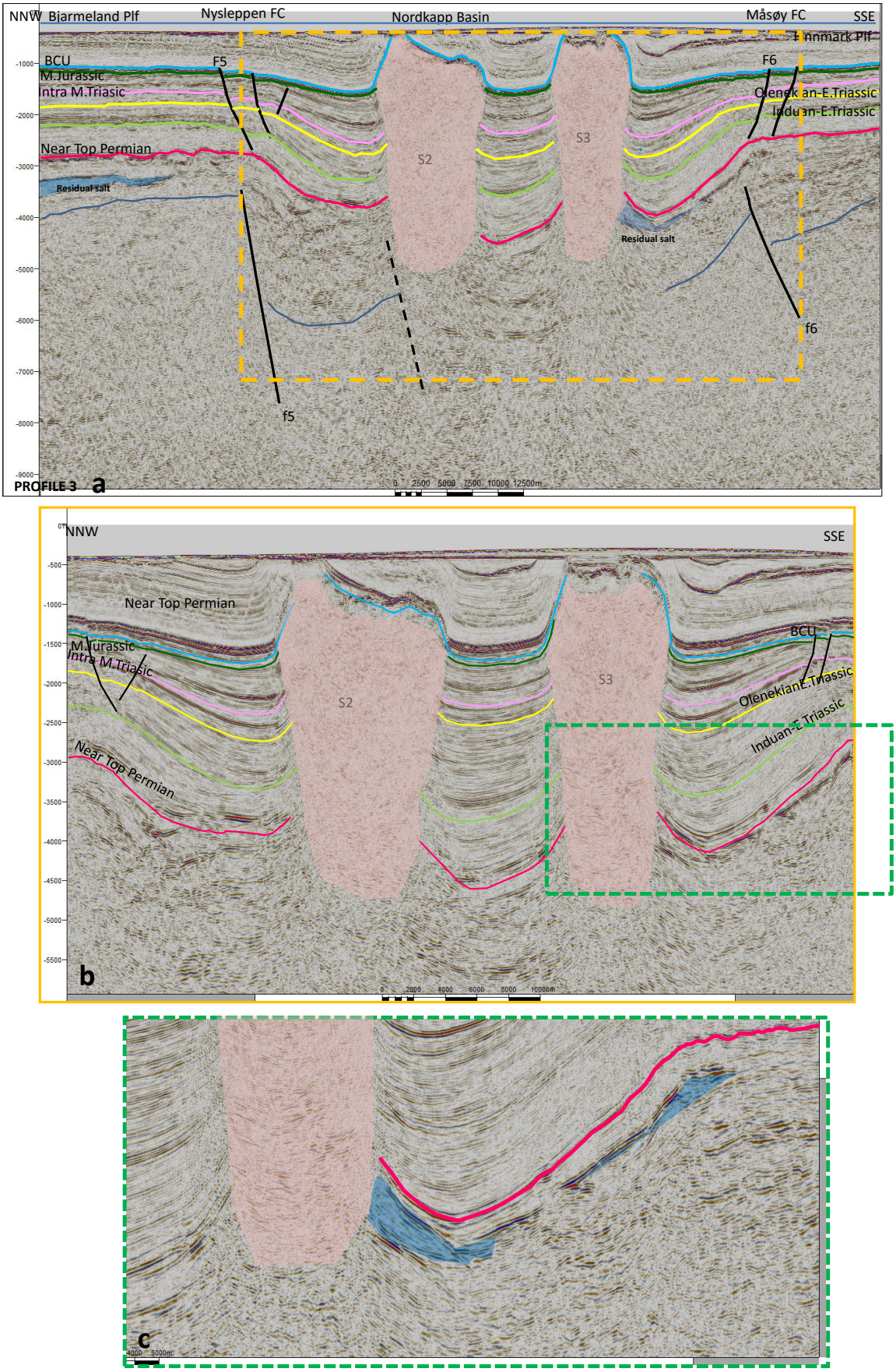

Figure 4. 4 Profile 3 transects the central part of the Nordkapp Basin which is strongly affected by salt diapirism with two salt diapirs present in the center of the basin. Diapirs are marked by transparent pink color.

Key profile 4

Profile 4 is a NW-SE seismic line. The line crosses through the well 7228/9-1 on the Finnmark Platform located in the southeasternmost part of the section (Figure 4.3).

The faults f5 and f8 at pre-salt level are similar to those which are observed in previous profiles. They are normal faults with a planar configuration. Both of them dip towards the SE. While the trend of f5 is NE-SW, the strike of fault segment f8 is more likely N-S (Figure 4.3).

Fault F7 of the Nysleppen Fault Complex has a trend of NE-SW (Figure 4.3). F7 is a normal fault with the dip-direction being SE. It has a listric geometry. Its vertical separation is around 0.015 s (Figure 4.7a). Fault F8 is normal and planar. Its strike is NW-SE. It has the opposite dip-direction with fault F7 (Figure 4.7a). In addition, it has a larger vertical displacement of 0.25 s as compared to other faults at the same level. Reverse drag of the sediment from Induan (Early Triassic) to Base Cretaceous on the hanging wall of the fault is observed. Small faults are also observed. Furthermore, the sediments on the footwall of the fault are uplifted (Figure 4.7b). It is an evidence of rotated faults.

The salt wall S4 is located in the center of the basin. It is closer to the Nysleppen Fault Complex at the northwestern margin than the Måsøy Fault Complex at the southeastern margin. It has a widening shape with the large ratio of the bulb (the widening part) to the stem. Its stem is nearly pinched out. It is 8 km in width and 15 km in length. Its strike is NNE-SSW. The salt wall intruded near to the seabed. Its crest is nearly emergent or thinly covered (Figure 4.7a). The geometry and characters of the rim syncline sequence is similar to that in the profile 1 (Figure 4.4). However, thinning in thickness of the Near Top Permian – Induan sequence in the area adjacent to the salt wall is observed.

A salt pillow (P3) is situated at the southeastern margin of the basin (Figure 4.7). The pillow is associated with the Måsøy Fault Complex. The top and base of the pillow is characterized by strong reflections. The base is a flat reflection at approximately 3.2 s. It has an asymmetric shape. It has the largest thickness at the crestal points of the pillow, which is roughly 0.5 s. It pinches out towards the east and the west. There are parallel reflections inside the pillow at the SE part of the profile. It is related to changes in evapporite minerals. The layers at the crest of the pillow are affected by a reverse fault. In addition, at base of the salt pillow, a small reverse fault is identified. Two other smaller salt structures lying towards the basin connect to the main pillow. It has concordant contact with the sediment below and above (Figure 4.7b).

The sediments along the basin margin were affected by the salt pillows. The layers below these two small pillows are deformed into curved layers. The Near Top Permian has a concordant contact with the top of the main salt pillow. Along the basin margin, a slightly thinning of the Induan (Early Triassic) to Middle Jurassic sequence is observed (Figure 4.7b).

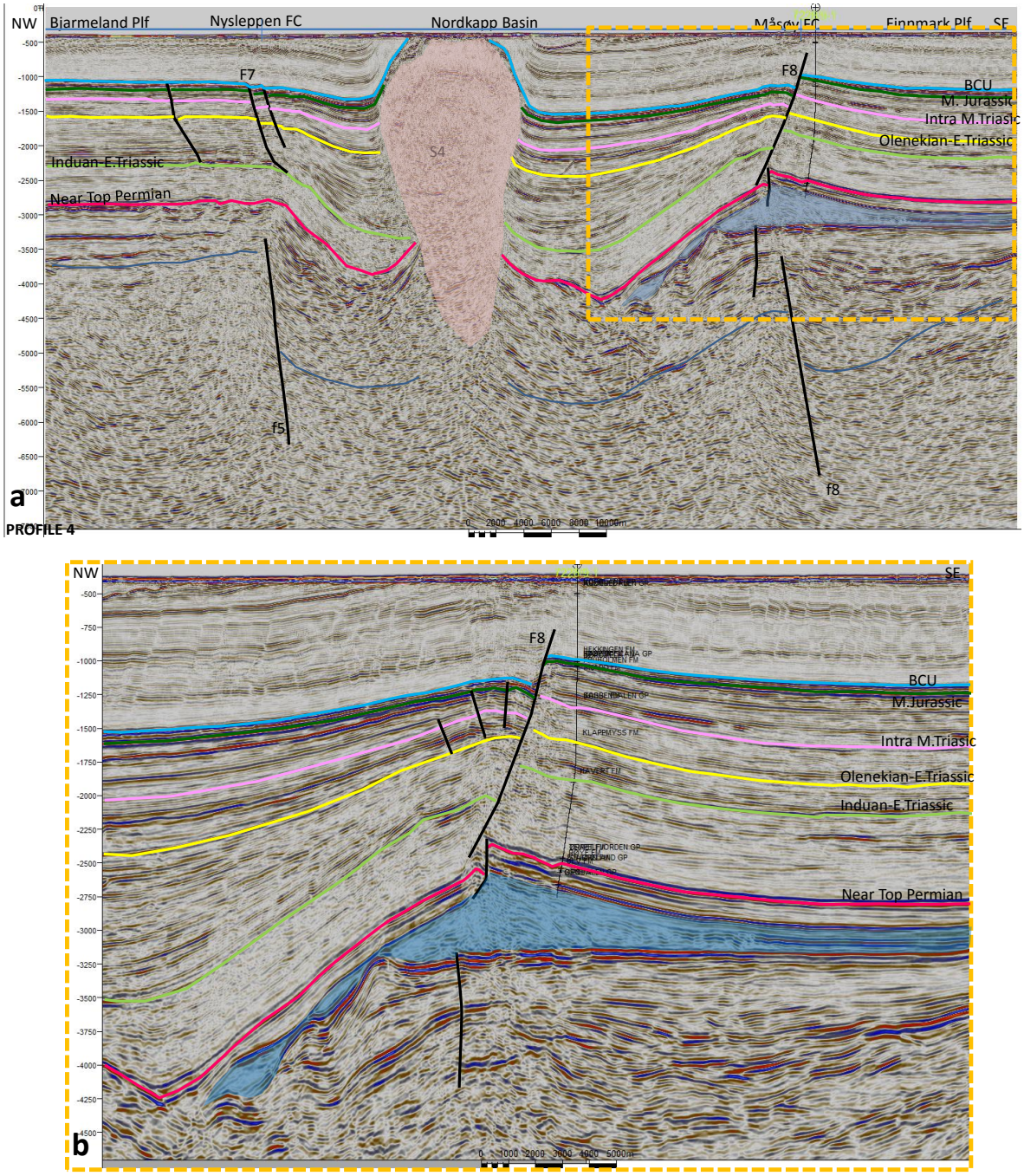

Figure 4. 5 Profile 4 with the NW-SE trending crosses through the well 7228/9-1 on the Finnmark Platform.

Table 4.3 summarizes information of fault segments of the Nysleppen and Måsøy fault complexes at the pre-salt level and the Base Cretaceous level.

	NAME	TYPE	TREND	DIP	THROW (ms TWT)	LEVEL	COMMENT
Nysleppen Fault Complex	f1	Normal, planar	NE-SW	SE	~ 1500	Pre-salt sedimentary level	Boundary fault
	f3	Normal, planar	NE-SW	SE	~ 2250		
	f5	Normal, planar	NE-SW	SE	~ 2000		
	F1	Normal, listric	NE-SW	SE	~ 40	Base Cretaceous level	Boundary fault
	F3	Normal, listric	NE-SW	SE	~ 100		
	F5	Normal, listric	NE-SW	SE	~ 120		
	F7	Normal, listric	NE-SW	SE	~ 15		
Måsøy Fault Complex	f2	Normal, planar	ENE-WSW	SE	~ 250	Pre-salt sedimentary level	Boundary fault
	f4	Normal, planar	ENE-WSW	SE	~ 500		
	f6	Normal, planar	ENE-WSW	SE	~ 700		
	f8	Normal, planar	NEN-SWS	SE	~ 600		
	F2	Normal, listric	ENE-WSW	NW	~ 60	Base Cretaceous level	Boundary fault
	F4	Normal, listric	NE-SW	NW	~ 80		
	F6	Normal, listric	NEN-SWS	W	~ 40		
	F8	Normal, planar, rotated	NW-SE	NW	~ 250		

Table 4. 3 Detailed description of fault segments in the study area.

4.5.3 Time-structure maps and time-thickness maps

Following are the time-structure maps of the two main horizons, Base Cretaceous Unconformity and Near Top Permian. The time-thickness map was also generated for a better understanding of change in sediment thickness through the basin.

Time-structure map of Near Top Permian

Near Top Permian is the lower boundary of the sequence. On the Bjarmeland and Finnmark platforms, the time values of Near Top Permian experience little variation (Figure 4.8). It is affected by the presence of salt pillows at the margins of the basin. At the position where the salt pillows are located, it shows smaller values in comparison with the surrounding area. Time values indicate an asymmetrical geometry of the basin at Near Top Permian level. The

northwestern part of the basin witnessed a larger subsidence than the southeastern part. From the southeastern margin, the Måsøy Fault Complex, Near Top Permian dips gradually toward the area close to the northwestern margin, the Nysleppen Fault Complex. It created the depo-centers for younger sediments. They are close to the northwestern margin, the Nysleppen Fault Complex. The strike of the depocenters is parallel to the general trend of the fault complex, the NE-SW trend.

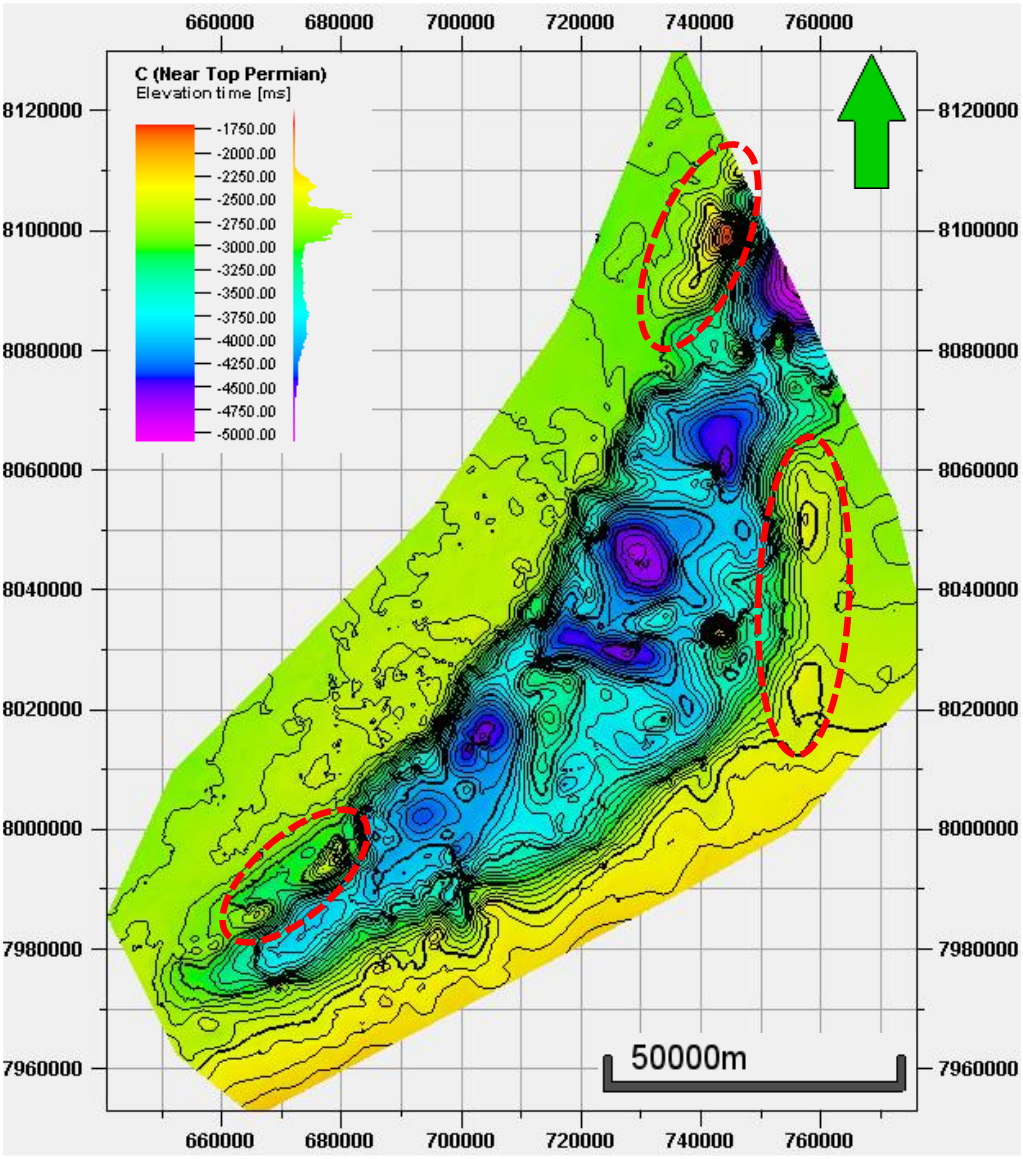

Figure 4. 6 Time-structure map of Near Top Permian with contour interval of 250 ms. Red ovals mark the position of salt pillows.

Time-structure map of Base Cretaceous Unconformity

The Base Cretaceous Unconformity is the upper boundary of the sequence. Similarly to Near Top Permian on the Bjarmeland and Finnmark platforms, Base Cretaceous Unconformity lies

nearly horizontally (Figure 4.9). Within the basin, the spacing of the contours shows that the time values of Base Cretaceous Unconformity undergo little variation except where the salt structures are present. The Base Cretaceous Unconformity is draped on the upper part of the salt structures. The map shows that the configuration of the basin is more symmetric than that at the Near Top Permian level (Figure 4.8).

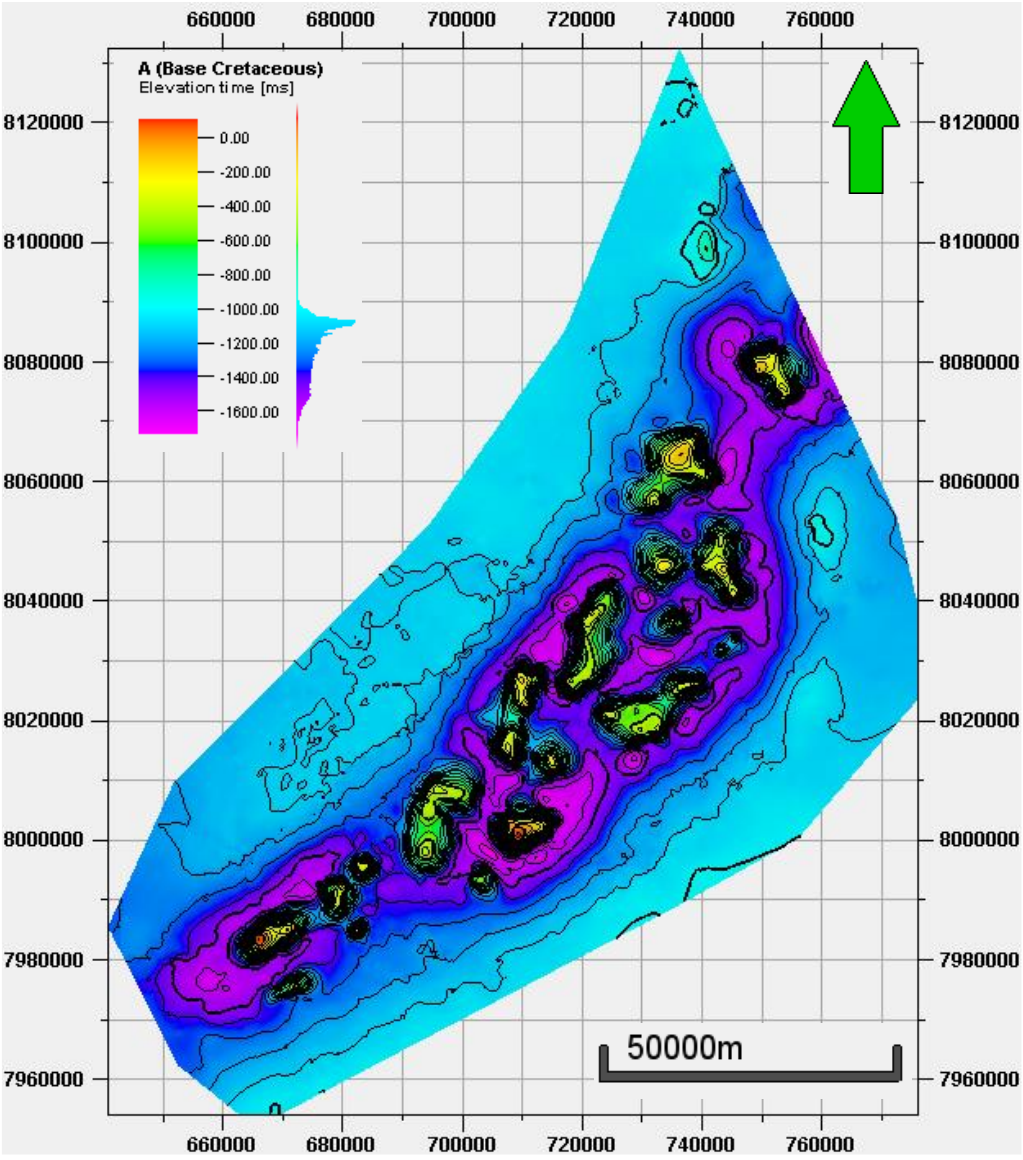

Figure 4. 7 Time-structure map of Base Cretaceous Unconformity with contour interval of 200 ms.

Time-thickness map of the sequence between Near Top Permian and Base Cretaceous Unconformity

The sequence has a relatively stable thickness on the Bjarmeland and Finnmark platforms (Figure 4.10). Within the basin, abnormal areas with high values of time-thickness and dense spacing of contours are related to salt structures. The thickness of the sequence increases

towards the salt structures. The abnormal areas are mostly closer to the northwestern margin of the basin, the Nysleppen Fault Complex than the southwestern margin. The different values of time-thickness of these areas demonstrate the difference in salt intervals. In addition, the location of three abnormal areas with smaller values of time-thickness in comparison with average values of time-thickness ion the platforms along the margins of the basin is associated with the salt pillows position. Moreover, the map indicates a ridge which separates the southwestern and northeastern sub-basin of the Nordkapp Basin. The ridge trends NW-SE (Figure 4.10).

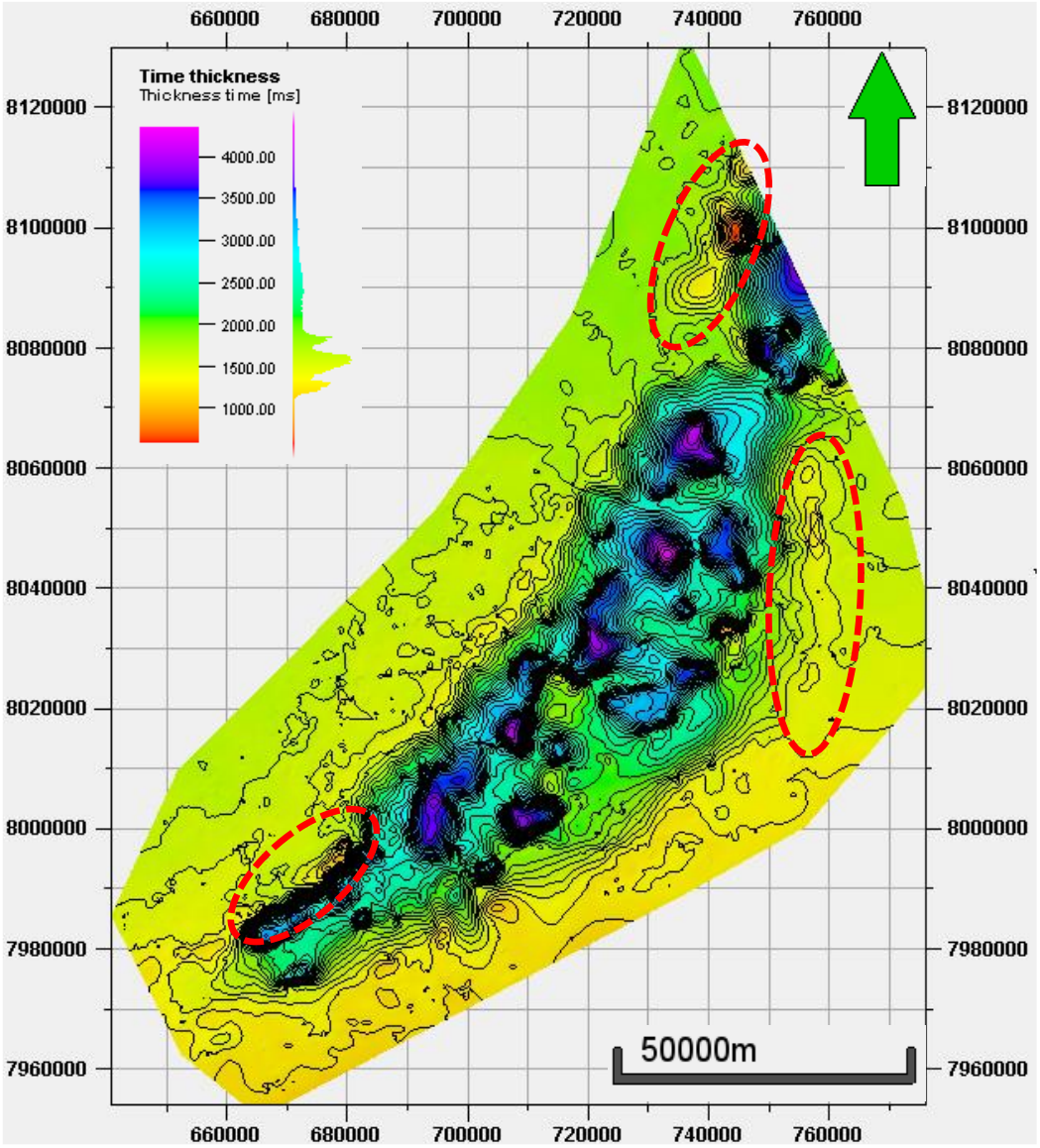

Figure 4. 8 Time-thickness map of the sequence between Near Top Permian and Base Cretaceous Unconformity with contour interval of 500 ms. The red ovals mark the position of salt pillows.

4.5.4 Salt distribution

The detailed observation of 2D seismic data indicates that the Base Cretaceous reflection was draped on the upper part of salt structures within the basin while the Near Top Permian reflection truncated against the salt structures (Figures 4.5, 4.5, 4.7). Hence, the time-structure map of the Base Cretaceous and the time-thickness map of the sequence between Near Top Permian and Base Cretaceous in combination with the observation in seismic sections can help to map out the distribution of salt structures within the basin. The outline of salt structures was mapped based on the contour of time-structure map of Base Cretaceous which shows that the reflection starts draping on the salt structures. It is usually characterized by the sudden increase of the density of contour lines.

Eighteen major salt walls and stocks were mapped in the basin (Figure 4.3). Salt structures observed from the study area similar to that from previous studies (Gabrielsen et al. (1992)**;** Jensen et al. (1992); Nilsen et al. (1996)**;** Koyi et al. (1993)). The salt walls are elongated along the strike of the basin (NE-SW orientation). Moreover, they are situated closer to the basin margin in the northwest, the Nysleppen Fault Complex, compared to that of the southeastern margin, the Måsøy Fault Complex (Figure 4.3). Rim synclines are located close to the salt diapirs with the axis parallel to the strike of the structures. Three salt pillows located at the margin of the basin are also indicated.

The distribution of salt structures is compared to the time-structure map of Base Cretaceous and the time-thickness map of the sequence of Near Top Permian-Base Cretaceous (Figures 4.11, 4.12). A good correlation is shown. Salt structures are related to areas with anomaly small time-values of Base Cretaceous and anomaly large time-thickness values of the sequence of Near Top Permian-Base Cretaceous.

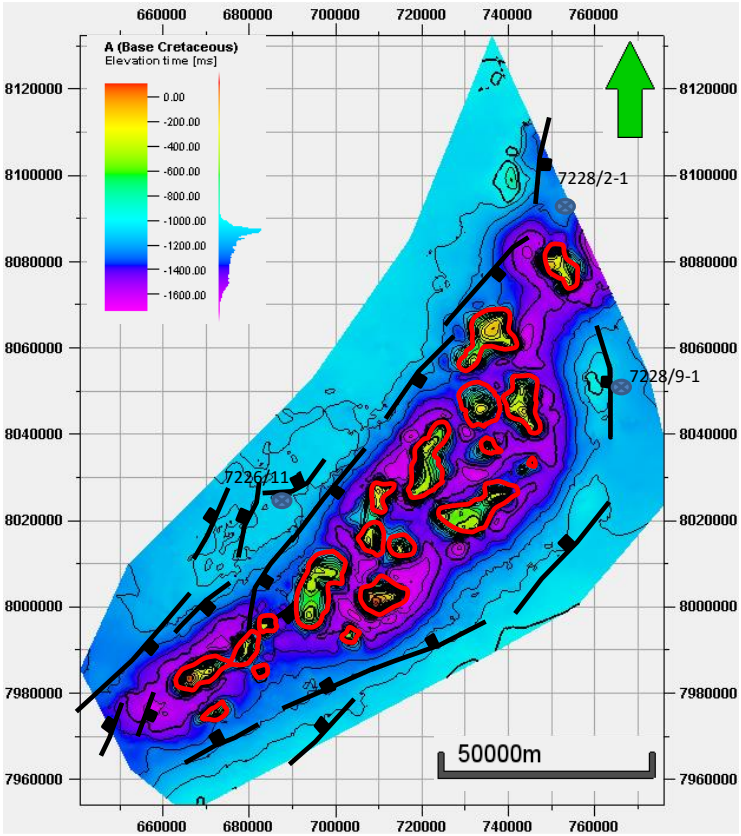

Figure 4. 9 The distribution of salt structures (red lines) within the basin compared to the time-structure map of Base Cretaceous.

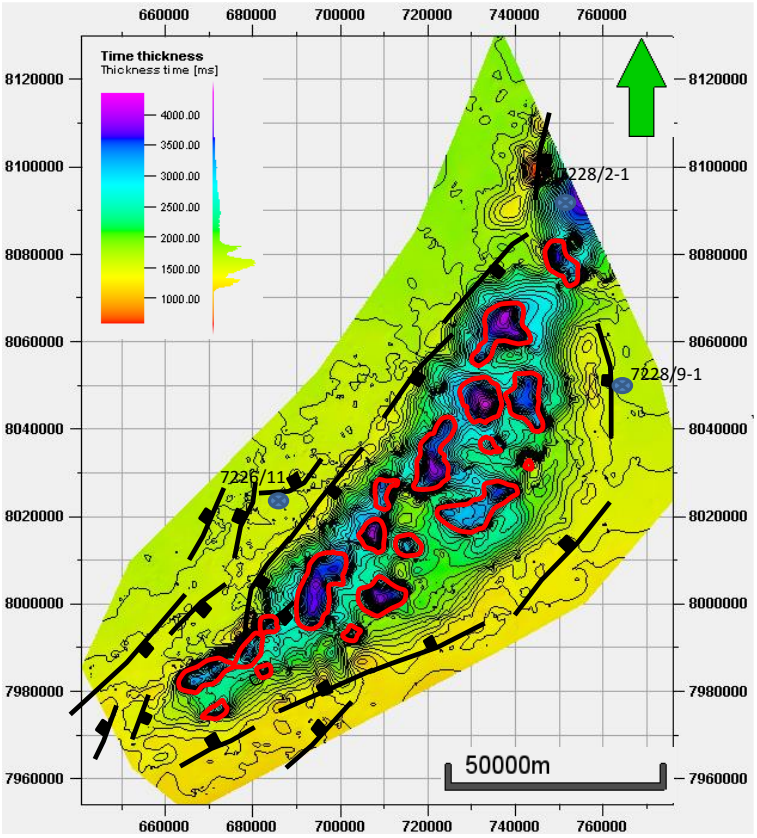

Figure 4. 10 The distribution of salt structures (red lines) within the basin compared to the time-thickness map of the sequence between Near Top Permian and Base Cretaceous.

Moreover, salt distribution from seismic interpretation is compared to filtered gravity anomalies (Figure 4.13). Salt gravitational signature is negative anomaly because of its low density in comparison with surrounding sedimentary rocks. The position of salt structures from two different methods has striking similarity. However, the map clearly shows that the outlines of salt structures do not match perfectly between two methods. The main reason is the uncertainty of interpretation and mapping method. Furthermore, salt pillows along the basin margins do not have such strong effect on gravity map as salt structures within the basin. This is because the salt pillows have a relatively low relief, so that the lateral density contrast is not of the same magnitude as for salt diapirs. These two independent geophysical methods together can provide a relatively good interpretation of distribution of salt structures.

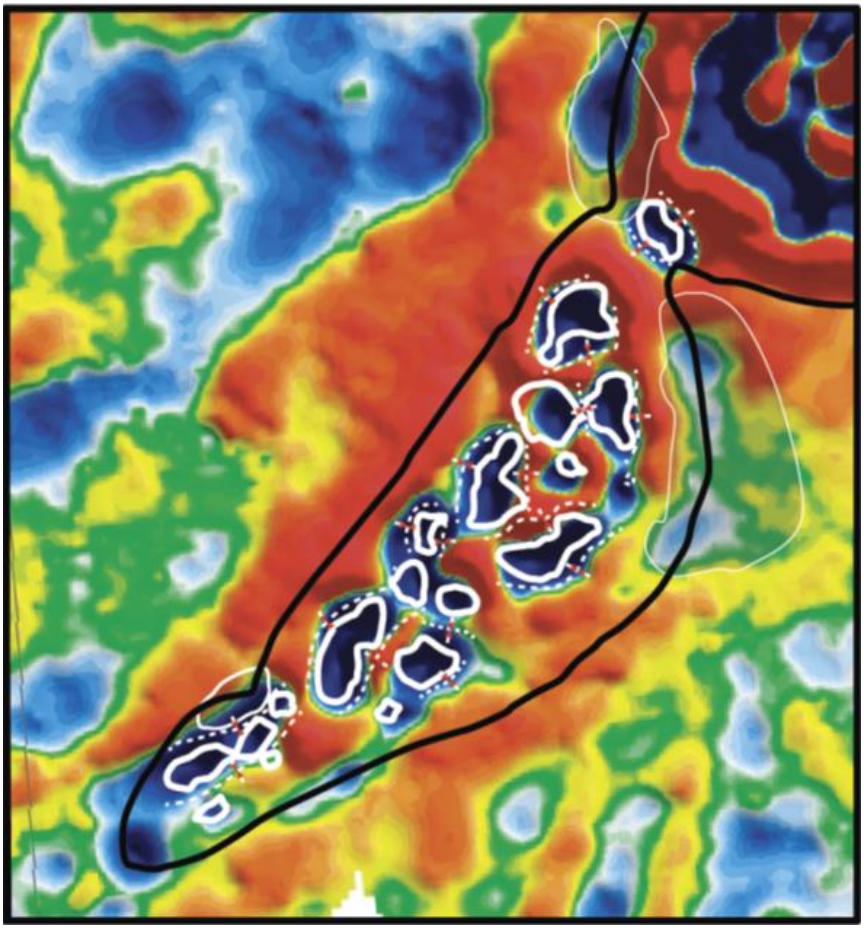

Figure 4. 11 Salt distribution from seismic interpretation compared to filtered gravity anomalies (Courtesy of TGS). White lines indicate the outlines of salt structures from seismic interpretation. Red color indicates positive gravity anomaly while blue color indicates negative gravity anomaly.

In addition, salt distribution from 2D seismic interpretation is compared to time-slices at 1500 ms and 3000 ms from a pseudo-3D seismic data cube which is provided by TGS (Figure 4.14). Time-slice at 1500 ms is close to the Base Cretaceous reflection while time-slice at 3000 ms is close to the Near Top Permian reflection within the basin. Homogeneous areas with no internal

reflections are corresponding to salt diapirs. Strong amplitude of reflections of the time-slice at 1500 ms enhances the contrasting seismic properties of salt and sediment. Hence, the image of salt structures is seen clearly. In general, because the distribution of salt structures is identified at the Base Cretaceous level, the map shows a better match of salt distribution with data in the time-slice at 1500 ms. The homogeneous area with no reflection is smaller in the time-slice at 3000 ms than at 1500 ms. It is an evidence of widening shape of salt diapirs within the basin. Moreover, salt pillows are not indicated in both two time-slices because of their position in vertical sections.

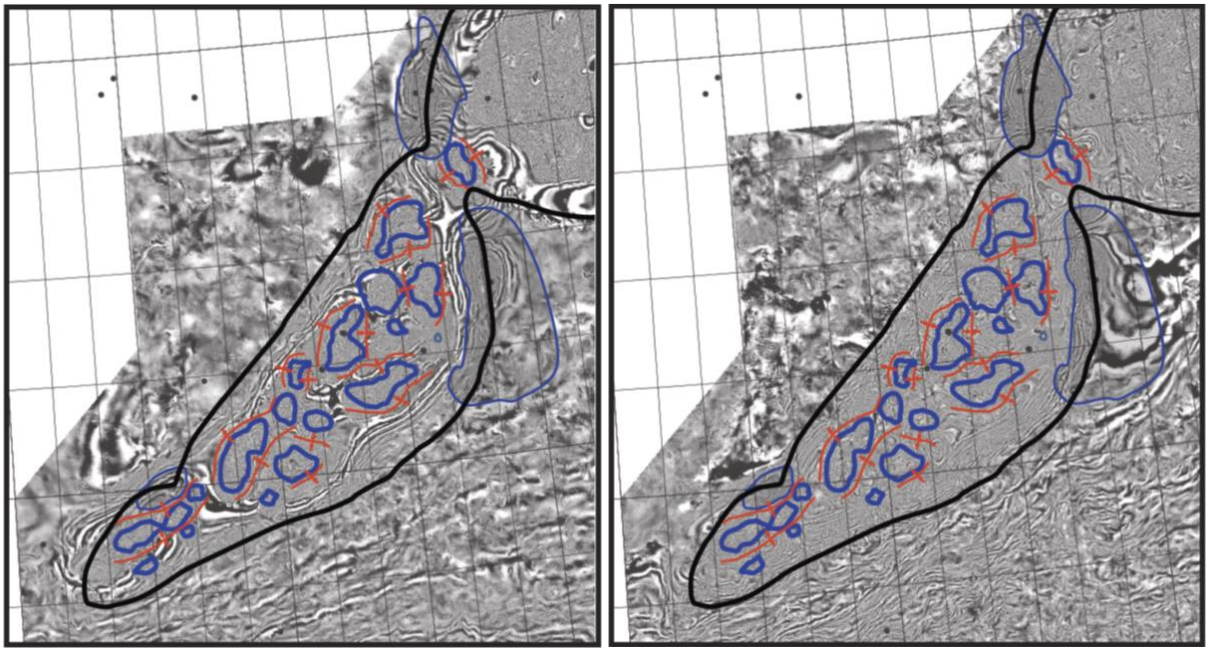

Figure 4. 12 Salt distribution from 2D seismic interpretation compared to time-slices at 1500 ms (left) and 3000 ms (right) from a pseudo-3D seismic data cube (Courtesy of TGS).Blue color indicates salt structure. Red color indicates rim syncline's axis.

4.5.5 Salt volume and thickness

Determination of the total quantity of salt in the SW Nordkapp Basin is performed based on the distribution of salt structures which results from 2D seismic interpretation. Firstly, all salt structures are numbered and calculate the area (Figure 4.15). The salt pillow P2 belongs to the NE Nordkapp basin, so it is not included in the calculation. The total areas of salt diapirs and salt pillows are 892 km^2 and 805 km^2, respectively.

Detailed observation in 2D seismic sections gives information of average height in two-way time of salt diapirs within the basin and salt pillows. The average heights are 4 s for salt diapirs and 0.3 s for salt pillows.

The formula used for volume calculation is applied for the cylinder shape which is the simpliest case here: Volume = area * thickness.

Salt diapirs have widening shape. Salt diapirs' area gets the largest number because the calculation is performed for the outcrop of salt diapirs at the top, the Base Cretaceous level. Hence, when calculating the volume of salt diapirs, a volume reduction for salt overhangs is included. Similarly, salt pillows have a triangular shape. An error when calculating the volume occurs. However, because the volume of salt pillows is much smaller than that of salt diapirs, the error is considered negligible. The detailed volume calculation is given below.

Volume of salt diapirs

Total area of salt diapirs: 892 km^2

Average height of salt diapirs (in twt): 4 s

Average velocity (Seabed-Top Permian): 4 km/s

Average height salt diapirs: 8 km

Volume reduction for salt "overhangs": 20 %

Total volume of salt diapirs: 5709 km^3

Volume of salt pillows

Total area of salt pillows (P1 + P3): 805 km^2

Average thickness of salt pillows (in twt): 0.3

Average velocity (salt): 5 km/s

Average thickness of salt pillows: 0.75 km

Total volume of salt pillows: 604 km^3

Total volume of salt: 5709 + 604 = 6313 km^3

The total salt volume in the SW Nordkapp Basin is estimated at approximately 6313 km^3. The spatial distribution or the basin area is estimated to be roughly 5141 km^2. Hence, the average

thickness of salt layer is given by dividing the salt volume of space. The result is approximately 1.2 km. It places an average thickness of salt sequence. Previous published estimates Jensen et al. (1992) suggested a salt thickness in the order of 2 km in the SW Nordkapp Basin. Consequently, it is difficult to control the uncertainties of this method.

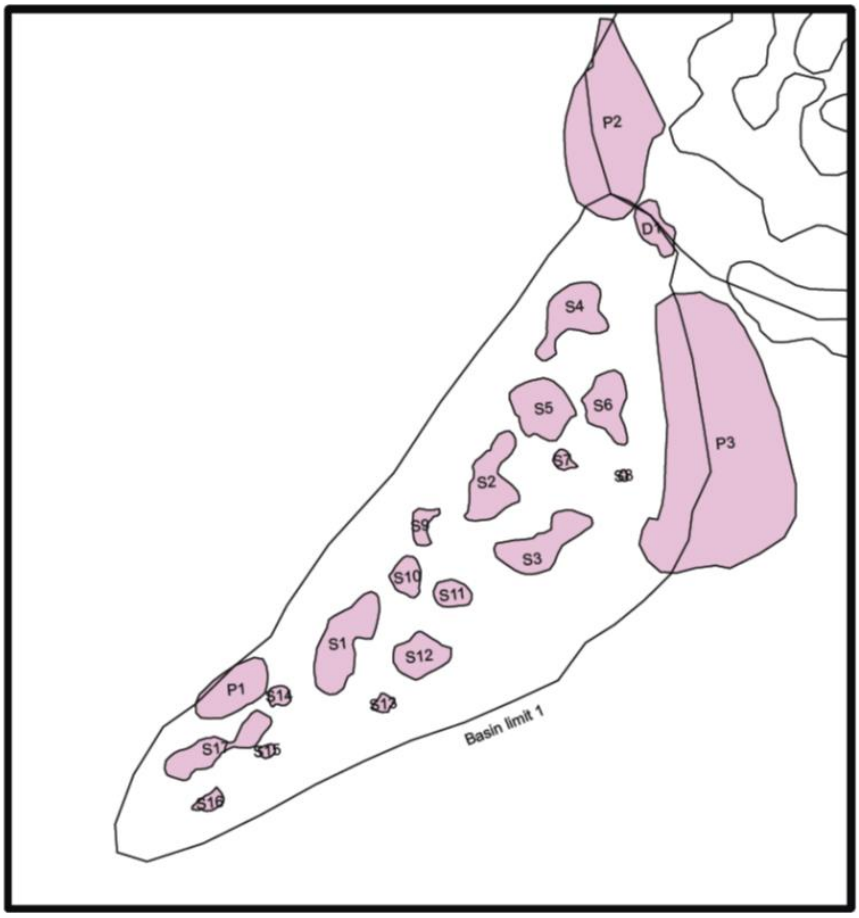

Salt_Name	area km^2
SW Basin limit (1)	5141
S1	115
S3	93
S5	91
S4	91
S2	89
S17	77
S6	69
S12	57
S10	30
S11	26
S9	20
S16	13
S14	11
S7	10
S13	9
S15	5
S8	2
D1	84
Total diapir	892
P1	89
P3	716
Total pillow (P1+P3)	805

Figure 4. 13 Salt structures labelled for use in volume calculation (left) and the result of area calculation (right).

5. DISCUSSION

This chapter focuses on the study of salt tectonics associated with tectonic evolution (fault activity and subsidence) of the southwestern Nordkapp Basin using results in the chapter 4.5, description of maps, key profiles and previous studies. This chapter will be divided into three main elements: 4.1 Basin configuration of the Late Paleozoic rift event; 4.2 Late Paleozoic evaporate and triggering mechanism for salt movement; 4.3 Stages of salt diapirsm; and 4.4 Basin configuration of the Jurassic rift event.

5.1 Basin configuration of the Late Paleozoic rift event

The Nordkapp Basin was formed with a general trend of NE-SW in the Late Devonian? – Carboniferous during the NW-SE directed extension in the Barents Sea (Gabrielsen et al. (1990); Faleide et al. (2010)). Reflection seismic data (chapter 4.4) show that this rift event was characterized by planar normal faults dipping towards the SE (fault system f) **(**Figures 4.4 – 4.7) (Figure 5.1b).

Salt deposits in the SW Nordkapp Basin make it difficult to define the deep basin configuration precisely here. For that reason, one seismic line through the part of the SW Nordkapp Basin which is not affected by salt diapirsim was selected to obtain a clearer image of the deep basin (Figure 4.1a). This section demonstrates that faults f1 and f2 are dip-slip faults facing in the same direction (SE). Faults of the Nysleppen Fault Complex, that defines the northwestern margin of the basin has a much larger vertical separation (2s TWT) compared with faults of the Måsøy Fault Complex, which coincides with the southeastern margin, compared with the Nysleppen Fault Complex (0.5s TWT; Figure 5.1a). The seismic velocity of the pre base Permian was estimated to be approximately 5.37 km/s on the platforms (Bergendahl, 1989). Hence, the vertical separations of faults are 5.37 and 1.34 km, respectively. Therefore, the Nordkapp Basin had a half graben configuration at the Late Paleozoic level with the larger subsidence along the northwestern margin.

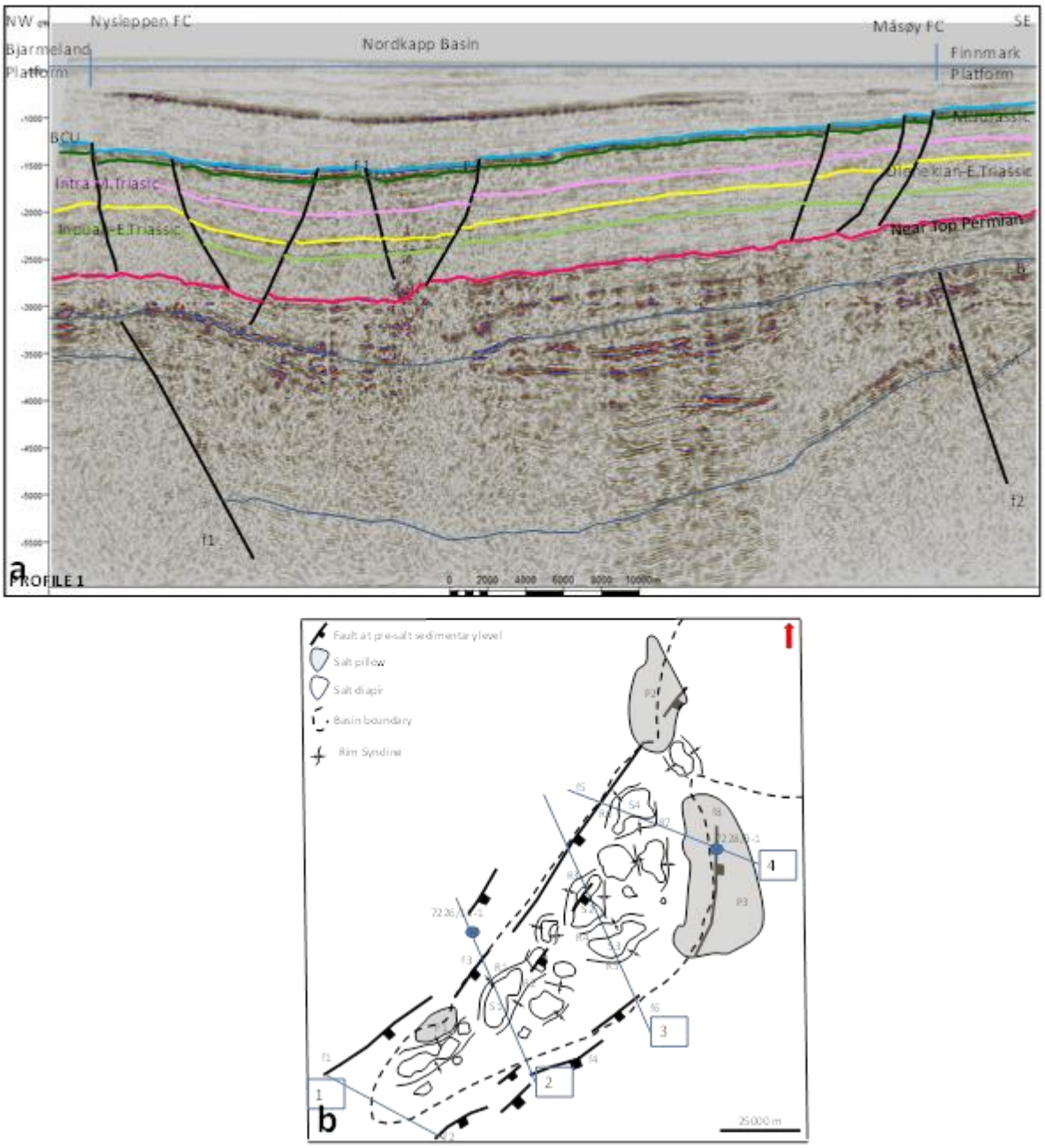

Figure 5. 1 (a) Profile 1 cross the part of the basin which is not affected by salt diapirism. (b) Map showing the fault distribution at the Paleozoic level and salt structures.

The growth and interaction of normal faults control not only the basin geometry. Also footwall uplift; hanging wall subsidence; erosion, transport and deposition of material; the source, drainage and accommodation space for sediment deposition are affected by this. Reflections A and B were selected in the profile 1 to constrain the geometry of the syn-rift sedimentary package. The reflection B is deemed to be the (erosional) base of a post-rift sequence due to that faults f1 and f2 cease at horizon B. In general, the sedimentary package between the reflections A and B has a wedge shape (Figure 5.1b). It is suggested that this basal geometry

was inherited in the later basin development so that the basin maintained the geometry with a thickness increase along the northwestern margin.

Figure 5.2 shows fault system of the SW Nordkapp Basin as the result of seismic interpretation in combination with the fault system of the NE Nordkapp Basin at Upper Devonian/Carboniferous level (Johansen et al., 1994). Master-faults are segmented. Half-grabens can be linked in various ways. They can be divided into two main families, including half-graben systems of opposing and similar polarity, respectively. Both families may consist of overlapping and non-overlapping half-grabens (Figure 5.3; Rosendahl et al. (1987)). This theory is applied to study the linkage between the SW part and the NE part of the Nordkapp Basin. The NW bounding faults of the SW part and the NE part of the Nordkapp Basin have similar polarity (Family 3, case G). They both face towards the SE. In contrast, the SE bounding faults of the SW part and the NE part of the Nordkapp Basin display opposite polarities. They do not overlap each other. The linkage between them can modelled by case E, Family 2 (Figure 5.3). This created a relatively un-subsided area between two sub-basins called an interbasinal ridge (Rosendahl et al., 1987).

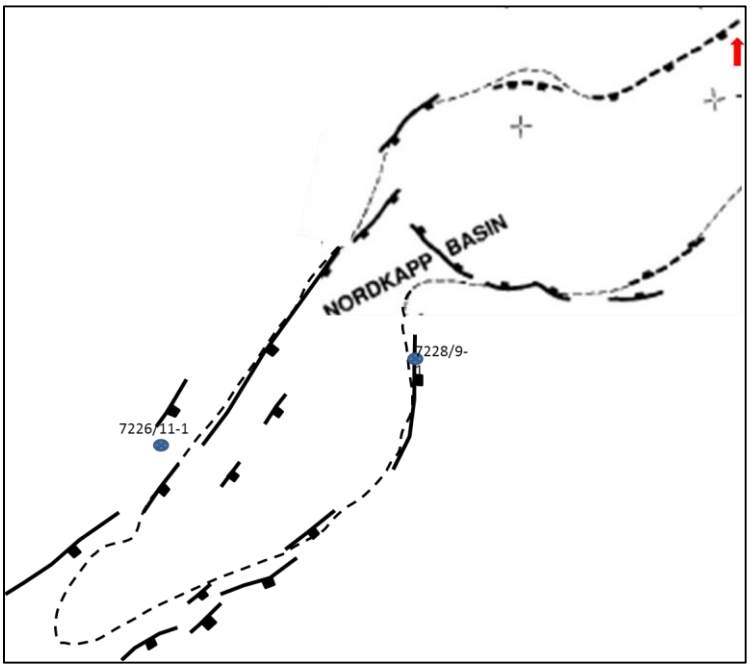

Figure 5. 2 The fault system at Late Devonian/Carboniferous level of the SW sub-basin from 2D seismic interpretation and of the NE sub-basin (Johansen et al., 1994).

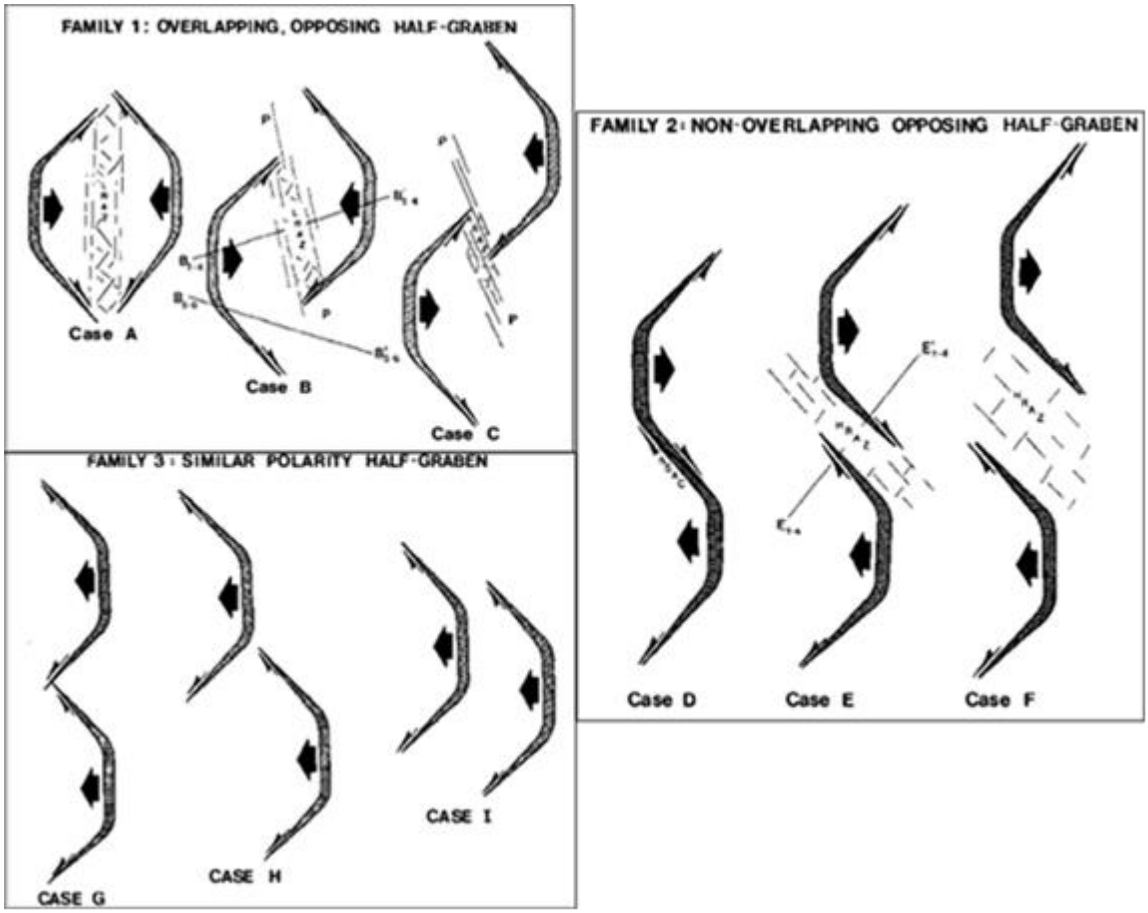

Figure 5. 3 Half--graben linkages groups into families (Rosendahl et al., 1987).

5.2 Late Paleozoic evaporites and triggering mechanism for salt movement

Calculation which was conducted in sub-chapter 4.5.5, suggests that there is a volume of evaporites of approximately 5709 km^3 associated with the salt diapirs in the center of the basin and 604 km^3 associated with the salt pillows at the basin margins. The calculation also shows that the average thickness of salt layer was approximately 1.2 km.

Due to the developing salt structures, the clastic sediment infill displays contrasting patterns in different parts of the basin (Figures 5.4a, b). Figure 5.4a illustrates constant sediment thickness of the Near Top Permian – Middle Jurassic succession in an area without halokinesis. In contrast, the Near Top Permian – Middle Jurassic succession of the SW Nordkapp Basin in the part which experienced the influence of salt movement shows the big variation in thickness (Figure 5.4b). Hence, it can help to identify the timing of salt movement.

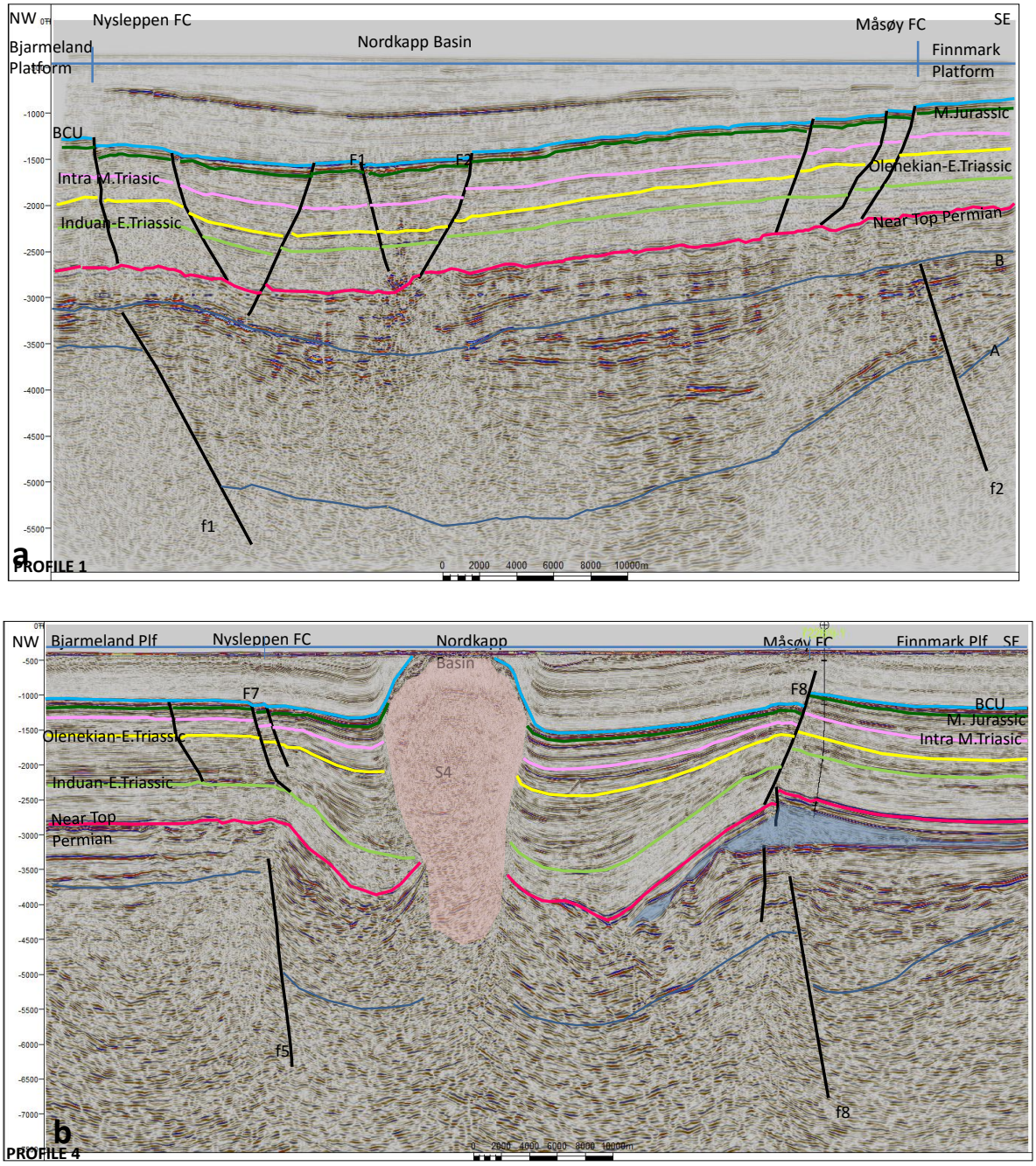

Figure 5. 4 The SW Nordkapp Basin infill sediment of Near Top Permian – Base Cretaceous succession which are illustrated through (a) a seismic line cross the part of the basin which is not affected by salt and (b) the part of the basin which is affected by salt.

The sequence between Near Top Permian and Induan-Early Triassic shows a clear thinning adjacent to the salt structure (Figure 5.5). According to the halokinetic model (Figure 3.5; Trusheim **(**1960**)**, it is suggested to be deposited in the primary rim synclines in the pillow stage of diapirism

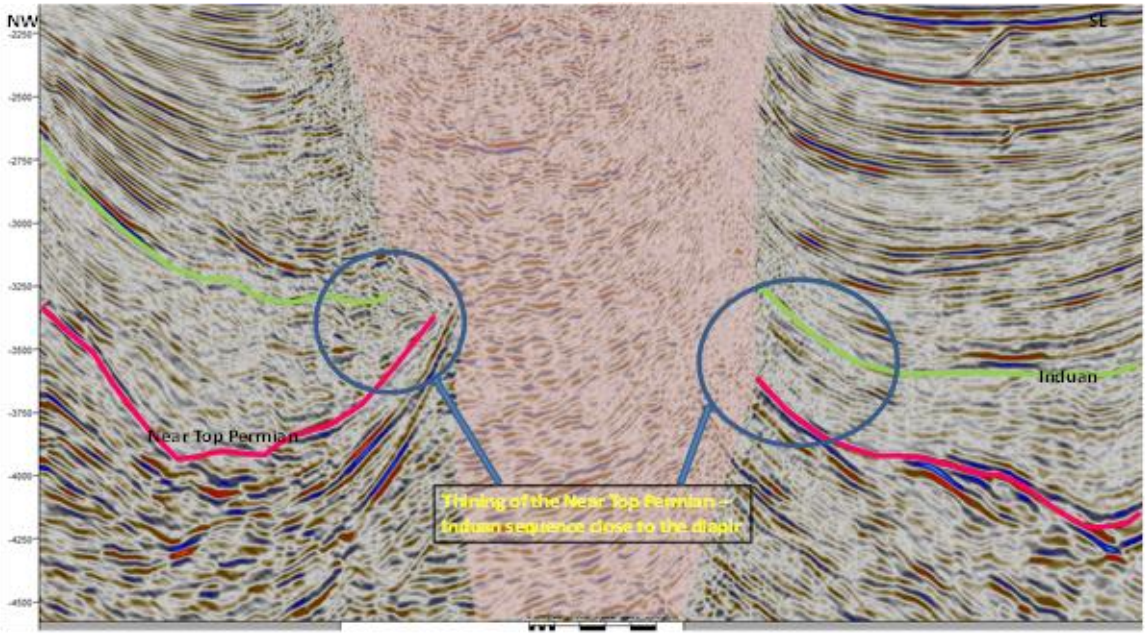

Figure 5. 5 Thinning of the sequence between Near Top Permian and Induan. The diapir is colored in light pink.

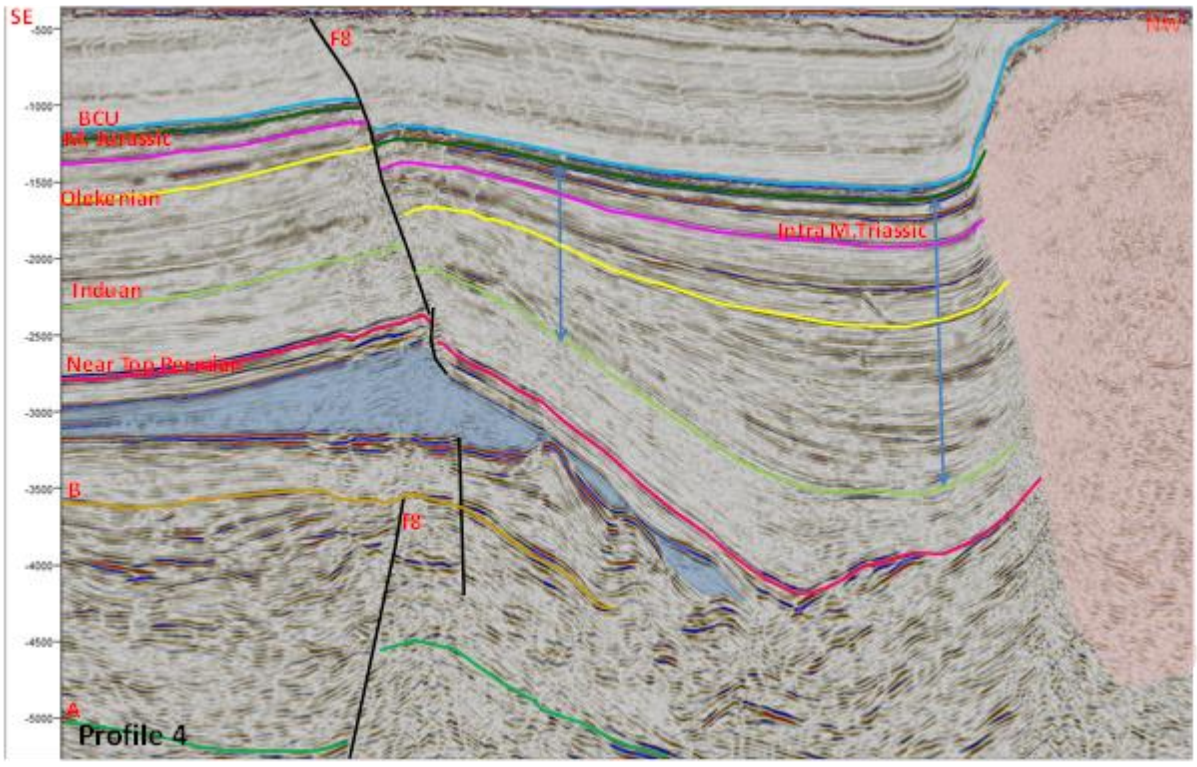

Figure 5. 6 A part of profile 4 showing the change in thickness of the Near Top Permian - Base Cretaceous package. Salt diapir is colored by light pink. Salt pillows are colored by blue.

Salt movement can be caused by many reasons which are discussed previously in chapter 3. Firstly, a presence of faults cutting through the sequence between Near Top Permian and Base Cretaceous is observed. It can be suggested that these fault could be active during a tectonic activity in Early Triassic and then be reactivated by later extension. However, no other evidence such as syn-tectonic deposited sediments is found to support this hypothesis. Hence, it is

unlikely that tectonic activity can be one of triggering mechanism for salt movement in the SW Nordkapp Basin. In addition, from observation on 2D seismic data, the sequence dated to Induan (Early Triassic) has a thickness of roughly 0.5 s TWT (figure 5.6). The average seismic velocity of Intra Lower Triassic is approximately 4.65 km/s (Bergendahl, 1989). Thus, the thickness of the sequence is calculated to be approximately 1160 m. The Induan lasted one million year. The sedimentary rate was 1.163 km/Ma. The clastic sediment of the Induan sequence was derived from the Uralian highland to the east (Figure 5.7; Faleide et al. (2010); Glørstad-Clark et al. (2010)). Therefore, a huge sediment source from the east came to the Nordkapp Basin with a high depositional rate. It, together with the overlying carbonate with high density created differential loading in the eastern part of the basin. It forced salt to move from the east to the west. Moreover, the basin had a half-graben geometry. It means that the salt movement, gravity sliding also happened due to the sloping configuration and supported for the salt movement (Figure 5.8). The origin salt layer of the SW Nordkapp Basin had larger thickness along the northwestern margin of the basin. When salt moved from the east to the west, the larger thickness of the mother layer along the northwestern margin enabled the salt buoyancy to overcome the strength of the overburden. Salt moved upwards. Therefore, salt structures are now situated closed to the northwestern margin, the Nysleppen Fault Complex. Consequently, differential loading is the most likely triggering mechanism for salt movement in the SW Nordkapp Basin. It was supported by gravity sliding.

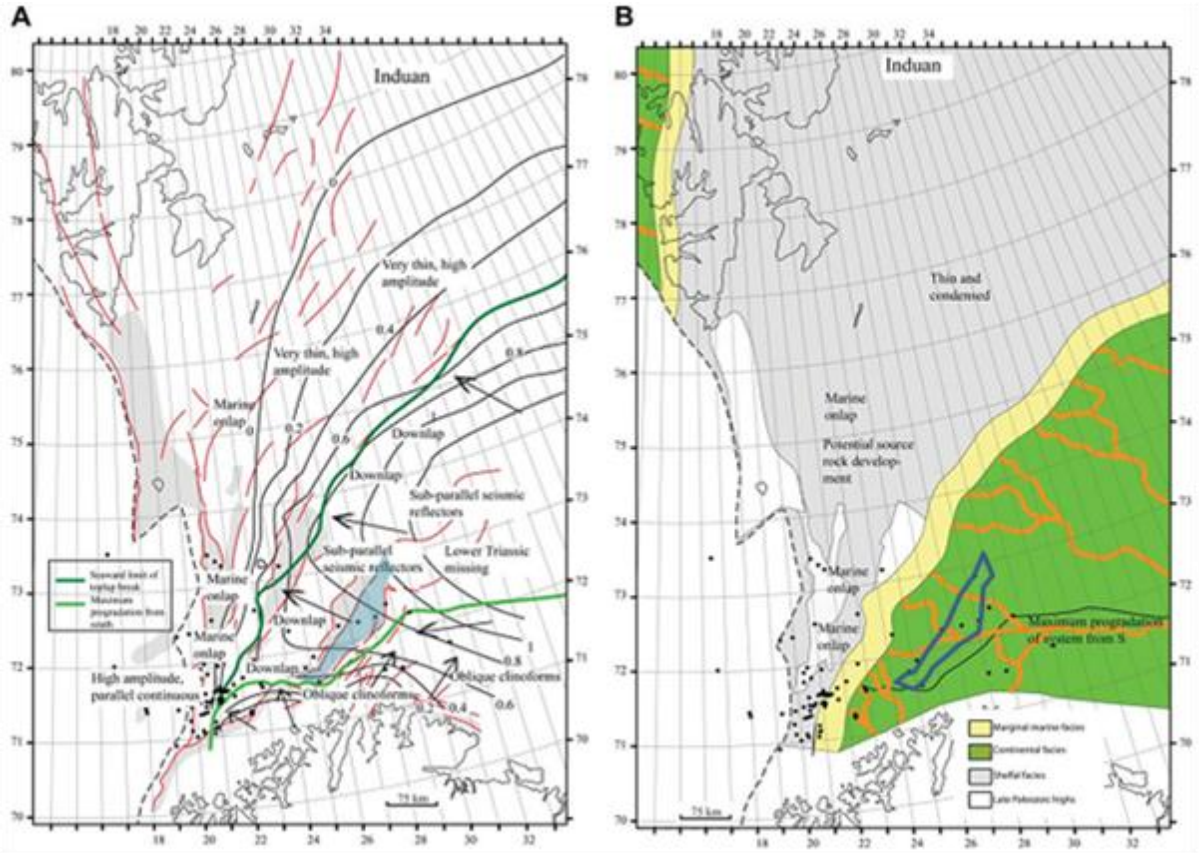

Figure 5. 7 Induan sequence time-thickness map (A) and Paleogeographic reconstruction of maxinum progradation with the sequence (Glørstad-Clark et al., 2010). The location of the SW Nordkapp basin are marked by blue color.

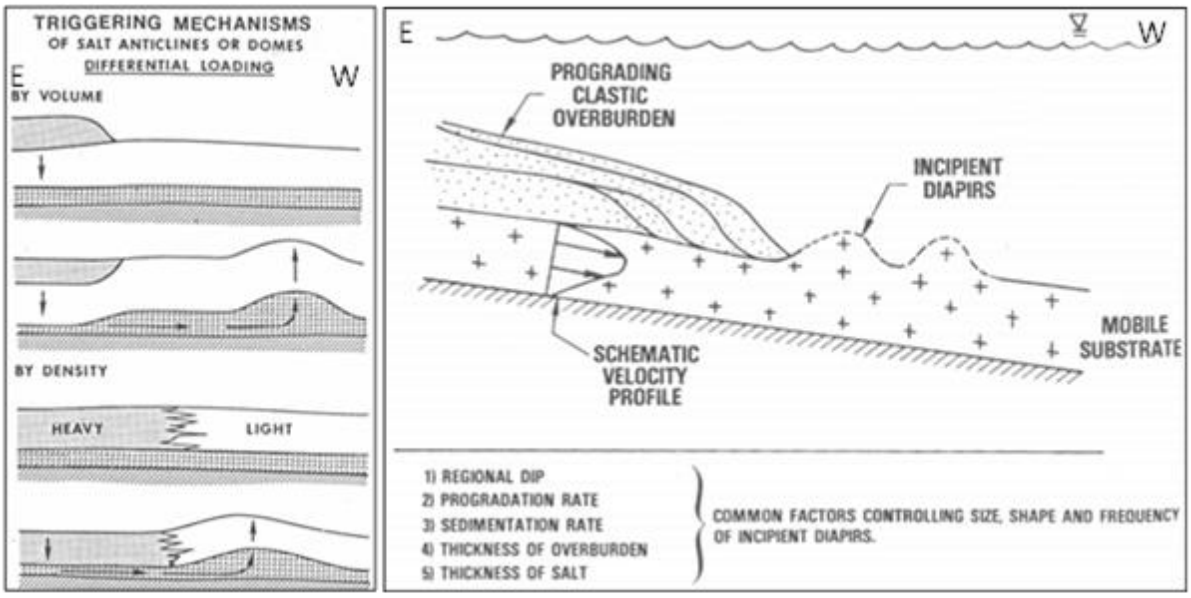

Figure 5. 8 Triggering mechanism is used to illustrate for salt movement of the SW Nordkapp Basin. Differential loading is the main mechanism and gravity sliding also supports the movement of salt.

5.3 Diapir stages

Based on the observation of sediment thickness variation in the SW Nordkapp Basin, it can be concluded that after the pillow stage which is suggested to happen in the Induan time-Early Triassic, the salt diapirism continued till Middle Jurassic time. It caused the increase in thickness of the succession towards salt diapirs (Figure 5.6).

The Olenekian (Early Triassic) was the main stage of salt diapirism because this sequence displays large sediment thickness variations, with thickness increasing in the direction of the salt structure and the divergent seismic reflection configuration within the sequence. Sediments of this age are also draped with sediments displaying a gentle dip along the flanks of salt structures. Significant withdrawal of salt from the source towards salt structures created large rim synclines that functioned as sediment traps around salt structures. Aggrading halokinetic sequence stacking is present. It is related to the vertical rise of diapir (Figrure 3.7). At the end of the period, the rate and amount of salt withdrawal decreased.

The Olenekian to mid Jurassic sequence has a smaller thickness variation (Figure 5.6). The sequence is characterized by sub-parallel reflections. Sediments of this age are draped with a higher dip along the flanks of salt structures. There is a presence of off-stepping halokinetic sequences stacking. These evidences indicate that it is the period that diapirs started expanding to have widening shape because the rate of salt growth is bigger than the rate of sedimentation (Figure 3.7).

The mid Jurassic – lowermost Cretaceous sequence marks a change in the history of diapirism. While Triassic sediment were truncated by the salt diapirs, mid Jurassic – lowermost Cretaceous sediments were passively draped across the diapirs. It together with the relatively constant thickness of the sequence indicate that no salt movement took place during this period. Salt can, however, be seen to intrude these strata during Cenozoic reactivation. However, the detailed study for this period was not carried out in this thesis.

The development of salt pillow along the basin margin likely happened at the same time as the development of salt diapirs within the basin because of slight thinning of Induan to Middle Jurassic sediment sequence towards the crest of salt pillows. The time thickness of the sequence close to the crest of salt pillow P3 (Figure 5.6) is approximately 800 ms, whereas the value at the position further towards the SE is roughly 900 ms. Therefore, when differential loading

occurred, along the basin margins, salt structures also developed because of the presence of thin layer of salt. However, they are in the pillow stage, the early stage of diapirism. It can be explained by the lack of salt supply. In contrast, the origin salt layer within the basin was much thicker than it along the basin margin. Hence, salt structures within the basin continued developing after the pillow stage.

5.4 Basin configuration of the Jurassic rift event

A rift phase started in Middle Jurassic as evidenced by wedge-shaped sediment packages in the hanging wall of master faults. It is characterized by normal master faults with listric configuration. The master faults consist of the master faults themselves and associated antithetic or synthetic subordinate faults. Master faults of the Nysleppen and Måsøy fault complexes have opposite dip-direction (Figure 5.9). Faults mostly splay and stop at the Near Top Permian. The vertical separation of these faults, which is just few hundred ms, is much smaller than that of deeply rooted faults (Figure 5.1). Smaller vertical separation of faults in compared with that of faults at Late Paleozoic level indicates the less bulk extension

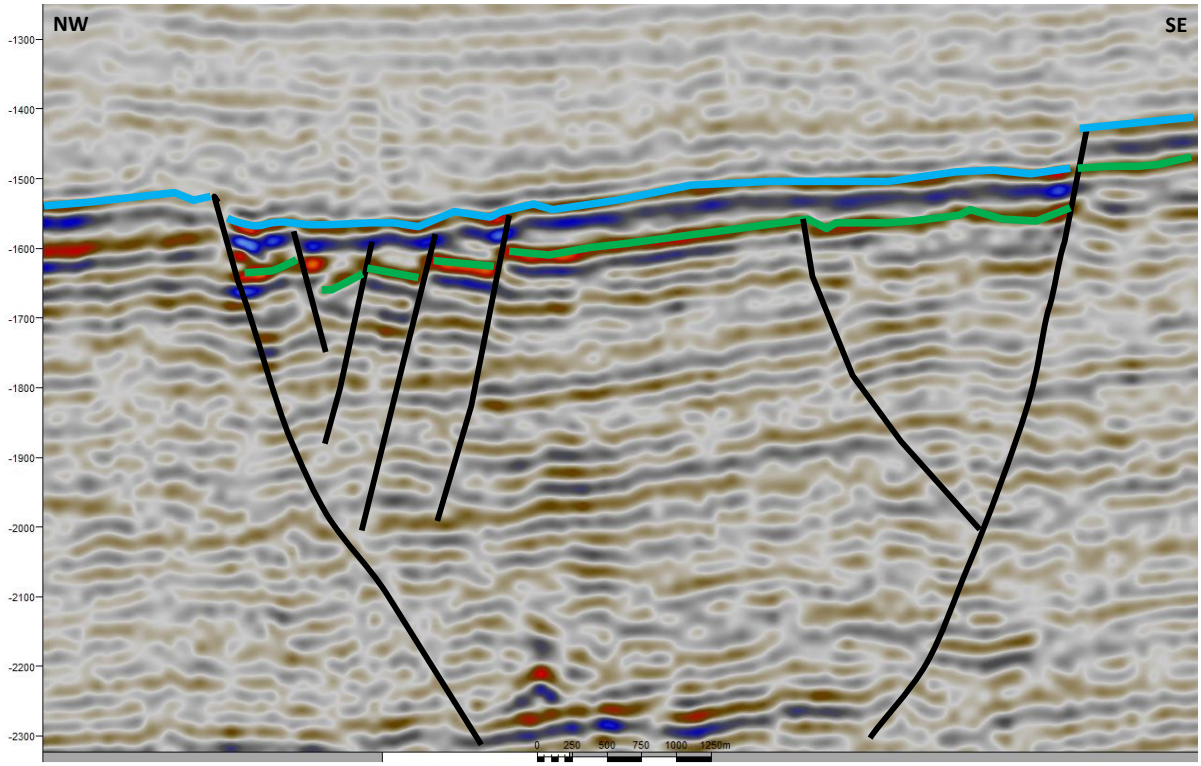

Figure 5. 9 A close zoom into the part of the SW Nordkapp Basin in the profile 1 indicating the rift event happening in Jurassic.

Figure 5.10 illustrates that the fault system at the Base Cretaceous level is more complicated than that at Late Paleozoic level and that the fault systems dip in opposite directions. The fault

zone of the fault group at Late Paleozoic is broader than that at Base Cretaceous, especially the southwesternmost part. The basin has a graben geometry which is symmetric and hence different to that seen at the Paleozoic level. Moreover, the linkage of the two sub-basins is different from the previous rift event. They have similar polarity. The differences in the basin configuration and the total width of faulted areas at the Late Paleozoic and Base Cretaceous levels can possibly be related to different width of the extended (thinned) lithosphere panel or to the depth of extension in the two cases.

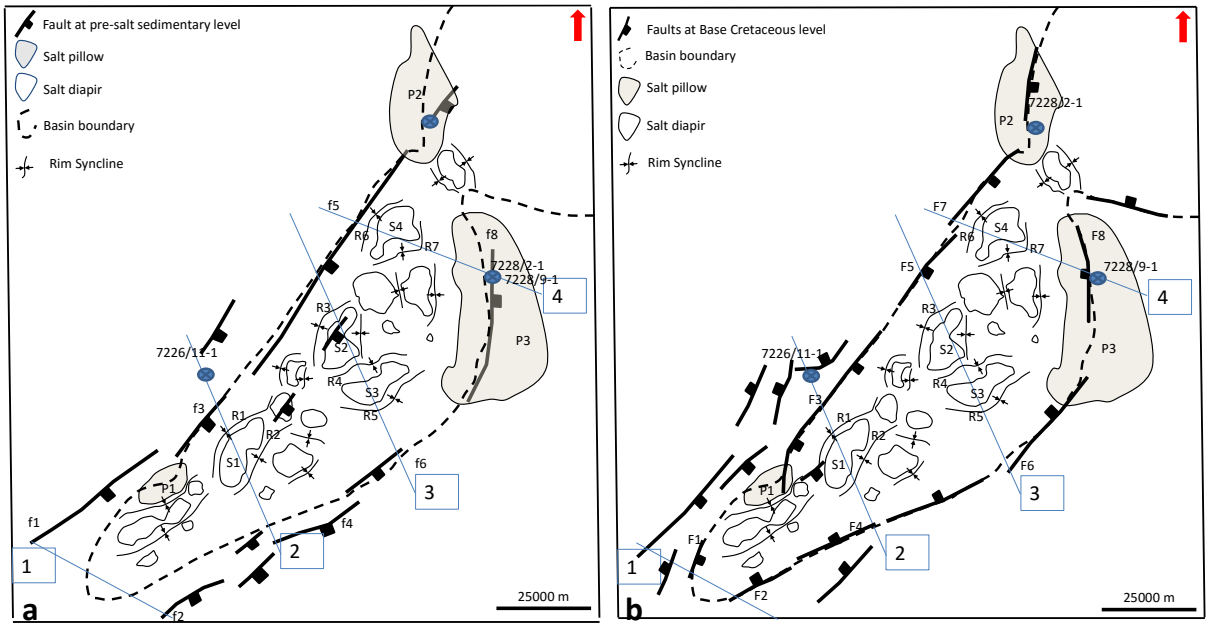

Figure 5. 10 Basin configuration at the Late Paleozoic level (a) and at the Base Cretaceous level (b).

Figure 5.11 Summary of the observation from sub-chapter 4.5 and timing of the main tectonic events in the SW Nordkapp Basin, the Nysleppen and Måsøy Fault Complexes from Paleozoic to Base Cretaceous time. It is based upon the results from interpretation and analysis of 2D seismic data in the study area.

The geological development of the SW Nordkapp Basin from the Late Paleozoic to Base Cretaceous is presented in the NW-SE trending schematic diagram (Figure 5.12).

	Fault		Sediment Package in the basin		Sediment package on the fault complexes and platforms	Salt movement	Tectonics
Period	Nysleppen FC	Måsøy FC		Thickness Variation			
Middle Jurassic – Base Cretaceous	- Lictric, normal faults - Vertical separation of few tens of ms TWT - General trend: NE-SW - 2 fault series: basin boundary faults dipping towards the NW and the other dipping towards the SE	- Lictric, normal faults - Vertical separation of few tens of ms TWT - General trend: ENE-WSW - Dip towards the SE	- No growth strata - Truncations at the Base Cretaceous - Wedge-shaped sediment package on the hanging wall of fault. - strata strongly folded following the upper part of salt walls	- Thickness variation on the hanging wall of fault	- Slightly variation of thickness: decrease toward the fault boundary.	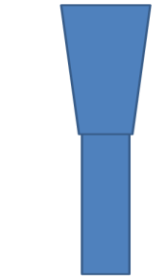 Pillow stage of salt diapirs within the basin	
Intra Middle Triassic – Middle Jurassic			- Growth strata strongly draped near the salt walls	- Small thickness variation - Small depocenters - Off-stepping sequence stacking	- Slightly variation of thickness: decrease toward the fault boundary.		
Olenekian (Early Triassic) – Intra Middle Triassic			- drape of growth strata to the flanks of salt walls				
Induan (Early Triassic) – Olenekian (Early Triassic)			- Gentle drape of growth strata to the flanks of salt walls	- large thickness variation: increase towards salt walls - large depocenter around sall walls - Aggrading sequence stacking	- Slightly thicker towards the fault boundary		
Near Top Permian – Induan (Early Triassic)				-- Thinning at the area adjacent to salt walls	- Concordant contact with salt pillow - Even thickness - Affected by reverse fault. Reverse drag on the hanging wall of fault.		
Pre salt (Late Palaeozoic)	- Planar, normal fault - Vertical separation of 1000 -2000 ms TWT - General trend: NE-SW - Dip towards the SE	- planar., normal fault - Active with vertical separation of ~ 500 ms TWT - Genal trend : ENE-WSW - Dip towards the SE	- Wedge-shape sediment package on the hanging wall of fault		- Sediment under salt pillow deformed - Affected by faults at the base of salt pillow		

Figure 5. 11 Summary of the observation from sub-chapter 4.5 and timing of the main tectonic events in the SW Nordkapp Basin, the Nysleppen and Måsøy Fault Complexes from Paleozoic to Base Cretaceous time. It is based upon the results from interpretation and analysis of 2D seismic data in the study area.

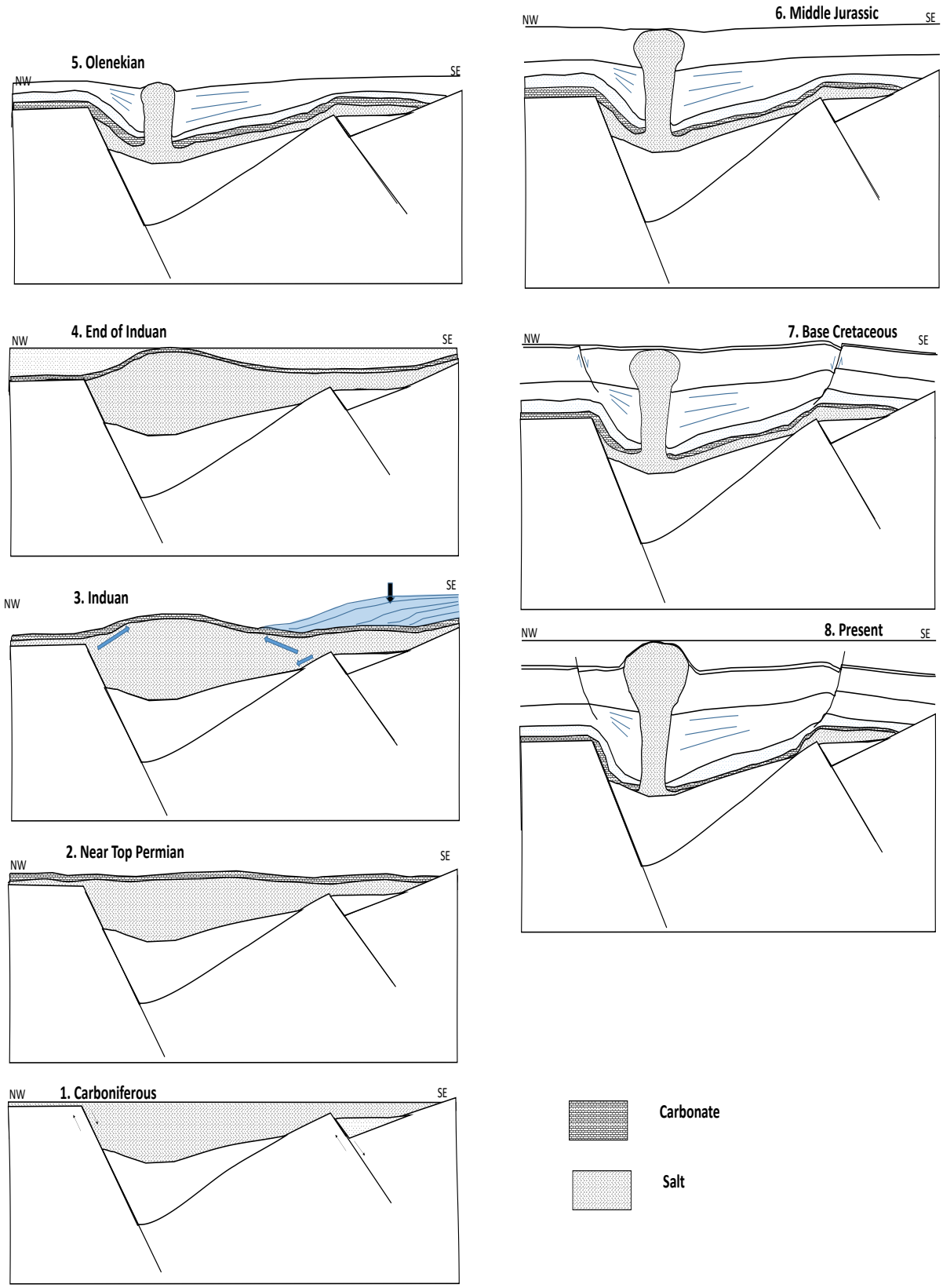

Figure 5. 12 Schematic diagram showing the geological development of the SW Nordkapp Basin until Base Cretaceous. The section is oriented NW-SE.

6. CONCLUSION

Based on the 2D seismic data and well data, detailed observation of sequence between Near Top Permian and Base Cretaceous Unconformity were carried out to identify salt structures and salt movement periods as well as its effects on sedimentary sequences in the SW Nordkapp Basin.

During the period of Late Paleozoic-Base Cretaceous, the Nordkapp Basin experienced two different rift phases: Late Paleozoic and Middle Jurassic-Base Cretaceous. The two rift phases have different magnitude and regime. It is represented by fault system and the configuration of the basin. Moreover, the later rift phase is partly affected by salt structures in the basin and along the basin margin. At the Late Paleozoic level, the rift phase created a half-graben with faults having large vertical separation. In contrast, the rift phase in Middle Jurassic-Base Cretaceous created a basin with a more symmetric configuration with two bounding fault series with opposite dip-direction. Faults along the margin where salt pillow is present are affected by salt pillows. They are rotated and curved in the map view.

A widespread evaporite layer was accumulated in the latest Carboniferous-earliest Permian time in the SW Barents Sea, including the SW Nordkapp Basin. The calculation indicates the original salt layer in the SW Nordkapp Basin had an average thickness of approximately 1.2 km. Based on obtained observation in 2D seismic data, salt is found in two structural settings:

- Stocks and walls in the basin: they are different in size and shape.
- Pillows along the margins of the basin.

Halokinetic evolution of the study area has been divided into:

- Near Top Permian – Induan (Early Triassic): It is called pillow stage with the thinning of the sequence in the area adjacent to salt structures within the basin. The upward movement of salt is a result of differential loading caused by the rapid deposition of a huge amount of clastic sediment from the north. Gravity sliding supported the movement of salt.
- Induan (Early Triassic) – Intra Middle Triassic: Large salt movement occurred. Salt withdrawal from the mother layer caused the depletion of overburden and created rim synclines which were filled by halokinetic sequences. Halokinetic sequences have

thickness increase towards salt structures. The ratio between the sedimentation rate and the salt growth rate is large. Salt pillows were formed along the margin of the basin at the same time.

- Intra Middle Triassic – Middle Jurassic: It is the late stage of halokinesis. The rate of salt growth exceeds the rate of sedimentation. Salt structures widened.
- Middle Jurassic – Base Cretaceous: Salt diapirsm was not active. The sequence has a relatively constant thickness. The sequence covered salt structures and were later truncated due to the reactivation of salt in the Cenozoic.

7. REFERENCES

ALSOP, G. I., BROWN, J. P., DAVISON, I. & GIBLING, M. 2000. The geometry of drag zones adjacent to salt diapirs. *J. Geol. Soc.*, 157**,** 1019-1029.

ARCHER, S. G., ALSOP, G. I., HARTLEY, A. J., GRANT, N. T. & HODGKINSON, R. 2012. Salt tectonics, sediments and prospectivity: An introduction. *Geological Society Special Publication,* 363**,** 1-6.

BERGENDAHL, E. 1989. Halokinetisk utvikling av Nordkappbassengets sørvestre segment. Oslo: Bergendahl, E.

BERGENDAHL, E. 1989. *Halokinetisk utvikling av Nordkappbassengets sørvestre segment : Vedlegg,* Oslo, Bergendahl, E.

DAVISON, I., ALSOP, G. I., EVANS, N. G. & SAFARICZ, M. 2000. Overburden deformation patterns and mechanisms of salt diapir penetration in the Central Graben, North Sea. *Marine and Petroleum Geology,* 17**,** 601-618.

DAVISON, I., ALSOP, I., BIRCH, P., ELDERS, C., EVANS, N., NICHOLSON, H., RORISON, P., WADE, D., WOODWARD, J. & YOUNG, M. 2000. Geometry and late-stage structural evolution of Central Graben salt diapirs, North Sea. *Marine and Petroleum Geology,* 17**,** 499-522.

EBBING, J., BARRÈRE, C., MARELLO, L., WERNER, S.C. 2009. Detailed crustal structure of the Barents Sea from 3D modelling. *Norwegian - Russian Arctic offshore workshop*.

EKERHEIM, S. B. & JOHANSEN, S. E. 2013. Regional geological seismic interpretation of Triassic infill in the southwestern Barents Sea. Institutt for petroleumsteknologi og anvendt geofysikk.

FALEIDE, J. I., BJORLYKKE, K. & GABRIELSEN, R. H. 2010. *Geology of the norwegian continental shelf*.

FALEIDE, J. I., BJØRLYKKE, K. & GABRIELSEN, R. H. 2015. *Geology of the norwegian continental shelf*.

FALEIDE, J. I., GNES, E. & GUDLAUGSSON, S. T. 1993. Late Mesozoic-Cenozoic evolution of the southwestern Barents Sea.

FALEIDE, J. I., GUDLAUGSSON, S. T. & JACQUART, G. 1984. Evolution of the western Barents Sea. *Marine and Petroleum Geology,* 1**,** 123,IN1,129,IN5,137-128,IN4,136,IN8,150.

FALEIDE, J. I., SOLHEIM, A., FIEDLER, A., HJELSTUEN, B. O., ANDERSEN, E. S. & VANNESTE, K. 1996. Late Cenozoic evolution of the western Barents Sea-Svalbard continental margin. *Global and Planetary Change,* 12**,** 53-74.

FOSSEN, H. 2010. *Structural geology,* Cambridge, Cambridge University Press.

GABRIELSEN, R., KLØVJAN, O., RASMUSSEN, A. & STØLAND, T. 1992. Interaction between halokinesis and faulting: Structuring of the margin of the Nordkapp Basin, Barents Sea Region. Structural and tectonic modelling and its application to petroleum geology. *Norwegian Petroleum Society*.

GABRIELSEN, R. H. & NORGE, O. 1990. *Structural elements of the Norwegian continental shelf : 6 : The Barents sea region,* Stavanger, Oljedirektoratet.

GILES, K. A. & LAWTON, T. F. 1999. Attributes and evolution of an exhumed salt weld, La Popa basin, northeastern Mexico. *Geology,* 27**,** 323-326.

GILES, K. A. & LAWTON, T. F. 2002. Halokinetic sequence stratigraphy adjacent to the El Papalote diapir, Northeastern Mexico. *AAPG Bulletin,* 86**,** 823-840.

GLØRSTAD-CLARK, EVY, FALEIDE, JAN INGE, LUNDSCHIEN, BJØRN ANDERS, NYSTUEN & PETTER, J. 2010. Triassic seismic sequence stratigraphy and

paleogeography of the western Barents Sea area. *Marine and Petroleum Geology,* 27**,** 1448-1475.
GUDLAUGSSON, S. T., FALEIDE, J. I., JOHANSEN, S. E. & BREIVIK, A. J. 1998. Late Palaeozoic structural development of the South-western Barents Sea. *Marine and Petroleum Geology,* 15**,** 73-102.
HANS, H. L. 1979. Seismic Recognition of Salt Diapirs: GEOLOGIC NOTES. *AAPG Bulletin,* 63.
HENRIKSEN, S. & VORREN, T. O. 1996. Early Tertiary sedimentation and salt tectonics in the Nordkapp Basin, southern Barents Sea. *Norsk geologisk tidsskrift,* 76**,** 33-44.
HUDEC, M. R. & JACKSON, M. P. A. 2007. Terra infirma: Understanding salt tectonics. *Earth Science Reviews,* 82**,** 1-28.
JENSEN, L. N. & SØRENSEN, K. 1992. Tectonic framework and halokinesis of the Nordkapp Basin, Barents Sea A2 - Larsen, R.M. *In:* BREKKE, H., LARSEN, B. T. & TALLERAAS, E. (eds.) *Structural and Tectonic Modelling and its Application to Petroleum Geology.* Amsterdam: Elsevier.
JENYON, M. K. 1986. *Salt tectonics,* London, Elsevier.
JENYON, M. K. 1991. ALTERNATIVES TO HALOKINESIS IN SALT DIAPIRISM. *Journal of Petroleum Geology,* 14**,** xi-xiv.
JOHANSEN, S. E., HENNINGSEN, T., RUNDHOVDE, E., SÆTHER, B. M., FICHLER, C. & RUESLÅTTEN, H. G. 1994. Continuation of the Caledonides north of Norway: seismic reflectors within the basement beneath the southern Barents Sea. *Marine and Petroleum Geology,* 11**,** 190-201.
KARE T. NILSEN, B. C. V. 1994. An Example of Salt Tectonics Controlled by Regional Tectonics: The Nordkapp Basin, Norway: ABSTRACT. *AAPG Bulletin,* 78.
KOYI, H. 1998. The shaping of salt diapirs. *Journal of Structural Geology,* 20**,** 321-338.
KOYI, H., JENYON, M. K. & PETERSEN, K. 1993. THE EFFECT OF BASEMENT FAULTING ON DIAPIRISM. *Journal of Petroleum Geology,* 16**,** 285-312.
KROKAN, B. 1988. Et gravimetrisk studium av nordkappbassenget. Oslo: B. Krokan.
LARSSEN, G. B., ELVEBAKK, G., HENRIKSEN, L.B., KRISTENSEN, S.E. 2002. Upper Palaeozoic lithostratigraphy of the southern Norwegian Barents Sea. *NPD-Bulletin No 9, Norwegian Petroleum Directorate*.
MARSHAK, S. & PROTHERO, D. R. 2001. *Earth : portrait of a planet,* New York, Norton.
MCGUINNESS, D. B. & HOSSACK, J. R. 1993. The development of allochthonous salt sheets as controlled by the rates of extension, sedimentation, and salt supply: Rates of geolical processes. *Gulf Coast Section SEPM 14th Annual Research Conference (127-139).*
NILSEN, K. T. 1995. Structural evolution and petroleum potential of the Norwegian Barents Sea. *AAPG Bulletin,* 79**,** 1240.
NILSEN, K. T. & JOHANSEN, J. T. 1996. Influence of regional tectonics on halokinesis in the Nordkapp Basin, Barents Sea. *AAPG Memoir***,** 413-436.
NPD. 2016. *Factpages* [Online]. Available: http://factpages.npd.no/factpages/ [Accessed 15/05 2016].
ROJO MORALEDA, L. A. 2015. Intepretation, modelling, and halokinetic evolution of salt diapirs in the Nordkapp Basin. University of Stavanger, Norway.
ROSENDAHL, B. & ROSENDAHL, B. 1987. Architecture of continental rifts with special reference to East Africa. *Annual Review of Earth and Planetary Sciences,* 15**,** 445-503.
SCHULTZ-ELA, D. D. 2003. Origin of drag folds bordering salt diapirs. *AAPG Bulletin,* 87**,** 757-780.
SMELROR, M., BASOV, V. A. & NORGES GEOLOGISKE, U. 2009. *Atlas : geological history of the Barents Sea,* Trondheim, Geological Survey of Norway.

STADTLER, C., FICHLER, C., HOKSTAD, K., MYRLUND, E. A., WIENECKE, S. & FOTLAND, B. 2014. Improved salt imaging in a basin context by high resolution potential field data: Nordkapp Basin, Barents Sea. *Geophysical Prospecting,* 62**,** 615-630.

TALBOT, C., KOYI, H. & CLARK, J. 1993. *Multiphase halokinesis in the Nordkapp Basin*.

TRUSHEIM, F. 1960. Mechanism of Salt Migration in Northern Germany. *AAPG Bulletin,* 44.

WOODBURY, H., MURRAY JR, I. & OSBORNE, R. 1980. Diapirs and their relation to hydrocarbon accumulation.

WORSLEY & DAVID 2008. The post-Caledonian development of Svalbard and the western Barents Sea. *Polar Research,* 27**,** 298-317.